TECHNIQUES FOR THE OPTIMIZATION OF THE RESISTANCE TO CAVITATION EROSION OF CERTAIN Cu-Zn AND Cu-Sn ALLOYS

PhD Thesis - Summary

for the award of the PhD degree
Polytechnic University of Timisoara
in the field of Mechanical Engineering

Author Eng. Iosif LAZĂR

PhD coordinators:: Univ.Prof.PhD.Eng. **Ilare Bordeaşu**
Univ. Prof..PhD.Eng **Ion Mitelea**

Timişoara

Month 4rd, Year 2020

TABLE OF CONTENTS
(extract)

1. PRELIMINARY LITERATURE RESEARCH ON THE USE OF COPPER-BASED ALLOYS IN THE PRODUCTION OF COMPONENTS SUBJECT TO CAVITATION WEAR

Copper-based alloys (brass and bronze) are largely used in the industry, due to their technological properties (to produce semi-finished components by casting, rolling, forging, due to their adaptability to mechanical processing and heat treatments, etc.), as well as for their physical and mechanical characteristics, which make them withstand the chemical corrosion during operation, as well as the thermal and hydrodynamic stress, such as cavitation.

Brass is a copper-zinc alloy which, depending on the number and percentage of alloy components and fillers (lead, tin, manganese, aluminum, iron, nickel), will display different properties, as follows: mechanical resistance, machinability, ductility, wear resistance, hardness, lack of brittleness in low temperatures, electrical and thermal conductivity, corrosion resistance [66], [67], [83].

Bronzeis a copper-tin alloy, largely used for cast component
Sometimes, the bronze semi-finished parts (such as the ones containing 4-8% tin) are forged, thus rendering them harder and more rigid than the forged brass alloys, being able to withstand high-velocity fluid flow (erosion-corrosion resistance).
Adding small quantities of phosphorus (0.01-0.45 %) further increases their hardness and their fatigue and wear resistance, and this makes them appropriate for the use in parts subject to thermal stress and cavitation, i.e. valves [67].

Below we will refer to the types of brass and bronze used in the production of ship propellers, and we will also briefly present the hydraulic machine components made out of these alloys.

a) Ship propeller with eroded blades (mounted on the stem)

b) Ship propeller in a vortex cavitation

Fig.1.5. Images of ship propellers made out of copper alloys] [72], [73]

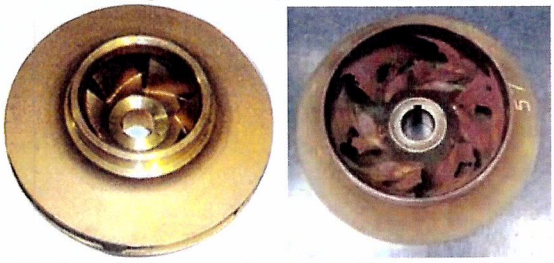

Before being put into service — Destroyed by cavitation

a) Bronze centrifugal pump rotor [71]

b) Centrifugal pump rotor with a common bronze stem, [72], [94]

Fig.1.13 Cavitation eroded centrifugal pump components

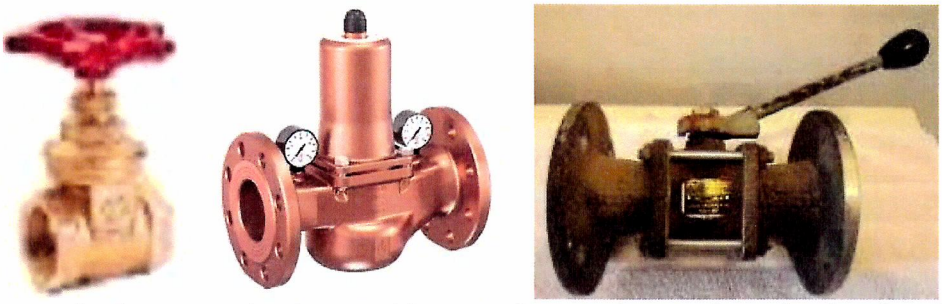

Fig.1.22 Bronze body taps and valves and brass or bronze (gate valve, check valve, ball valve)

Concluzie

We have noted a wide range of applications of copper alloys (brass, bronze) in the manufacturing of the most diverse parts (maritime and river boat propellers, hydraulic machine rotors, valves, taps, fittings, etc.) which operate in hydrodynamic environments with cavitation of various intensities, being eroded due to stress caused by the impact with the microjets and shock waves formed by cavitation bubble impingements.

The objectives of the Ph.D. thesis

The objectives of this thesis are as follows:

- research in the behaviour and resistance to vibratory cavitation of bronze (Cu-Sn) and of brass (CuZn39Pb3), used in casting the parts mentioned above, which are subject to cavitation erosion; these parts go through in-depth specific heat treatments, aimed at improving their behaviour and resistance to cavitation, as compared to their initial state, similar to other materials.
- research in the behaviour and deterioration process of the polymer resin layers, subject to vibratory cavitation;
- in-depth analysis of the deterioration process by cavitation erosion occurring at the surface of bronze and brass sample parts, subject to various types of in-depth heat treatments, as well as at the surface of the samples coated in polymer resins, by using a standard piezoelectric crystal assembly (with the following characteristics: T2 (vibration amplitude = 50 μm, vibration frequency= 20,000±1% Hz, sample diameter = 15.8 mm), available in the Cavitation Research Laboratory at the Polytechnic University from Timisoara;
- investigate the morphology and the macro- and micro-structural characteristics of the sample surfaces subject to cavitation erosion, using the latest optical and electronic equipment, and study the mechanism for the generation and propagation of cracking and tears;
- assess the obtained results, by comparing them with the results specific for the reference materials in the laboratory, using the specific curves and parameters recommended by the ASTM G32-2010 norms [56], as well as the images of the eroded micro-structure, obtained with an optical and an electron microscope.

The novelty of the Ph.D thesis

The novelty of this Ph.D consists in the fact that it identifies methods for the in-depth heat treatments that will improve the resistance to cavitation erosion of bronze (CuSn12) and brass (CuZn39Pb3), which are used to produce ship propellers, hydraulic pump impellers, components for valves and taps, as well as various fittings subject to cavitation. The research also focuses on the behaviour to vibratory cavitation of certain types of polymer resins, used to cover the surfaces of the bronze (CuSn12) samples subject to cavitation erosion.

2. MATERIALS, LABORATORY EQUIPMENT AND METHODS USED IN THE EXPERIMENTAL RESEARCH

1- Brass, provided by the company Color-Metal S.R.L.a bar-shaped sample, 20 mm in diameter that, besides zinc, also contains a main chemical element and lead. The chemical formula of this material, according to EN 10204:2004, is CuZn39Pb3.

The assays performed in the specialized laboratories within the Polytechnic University from Timisoara have resulted in the following values:

- Chemical composition: 57.7 % Cu, 38.49 % Zn, 3.3 % Pb, 0.2 % Fe, 0.1 % Ni, 0.2 % Sn, 0.01 % Al.
- Mechanical properties: tensile strenght R_m = 502 MPa, yield strength $R_{p0.2}$= 365 MPa, Brinell hardness = 115 daN/mm^2, breaking elongation A5 = 18 %, modulus of longitudinal elasticity E = 97 GPa, density ρ = 8.47 g/cm;
- the two-phase structure, made up of the solid solution and the electronic compound , fig.2.1, [1], [82].

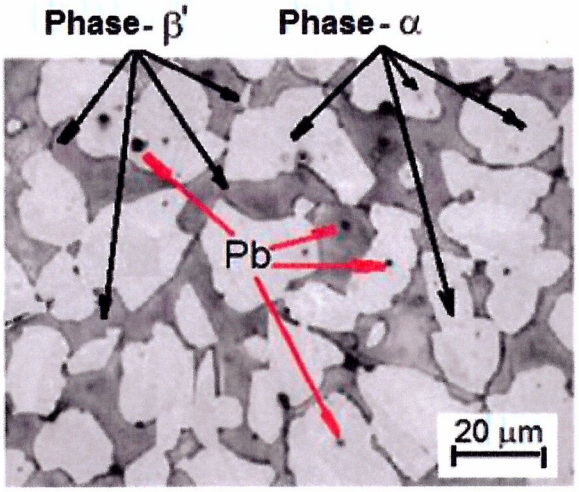

Fig.2.1 The structure of brass (CuZn39Pb3) (image taken from [82])

This two-phase structured brass (α with a c.f.c. grid and β' with c.v.c. grid),was chosen based on the fact that these types of brass are largely used in the production of pressure valve seats and of taps used in the propelling hydraulic systems [66], [90] which, in certain operational conditions are subject to a milder cavitation-erosion process.

1- Bronze is a Cu-Sn alloy, with Pb, Fe, Ni, and Zn content (chemical formula: CuSn12-C, according to the DIN EN 1982 standard), and it was chosen because it is recommended for use where the stress is higher and where wear and tear endurance in corrosion and cavitation conditions is more needed [38], [83];

The assays performed in the specialized laboratories within the Polytechnic University from Timisoara have resulted in the following values:

- Chemical composition:85.16 % Cu, 11.18 % Sn, 0.4856 % Zn, 0.7983 % Pb, 0.5226 % Fe, 0.6933 % Ni, 0.2 % Sn, 0.0304 % Mn, 0.0382 %S, 0.0714 %Sb, <0.003 %P;
- Mechanical properties: yield strength R_m = 312 MPa, fluid flow $R_{p0.2}$ = 157 MPa, ball hardness = 97 daN/mm^2, breaking elongation A5 = 9 %, modulus of longitudinal elasticity E = 97 GPa, density ρ = 8.77 g/cm
- the two-phase structure, made up of solid grain solution α and, in a higher tin content, of grain solution α and eutectoid grains (α + δ) [83], fig. 2.2.

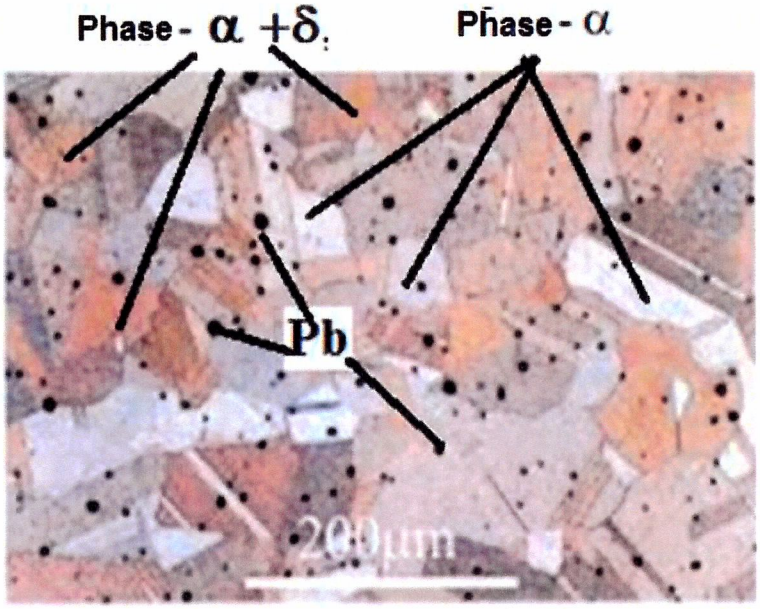

Fig.2.2 The structure of brass (CuSn12) (image taken from [84])

This type of bronze was chosen because it has shown a better endurance in salted water and, for this reason, it is still used to cast ship propellers.

Another reason for including this material in the research on cavitation erosion is related to its processing characteristics, such as high frictional resistance, long fatigue life, good machining, cold-age hardening, satisfactorily weldable and, most important, its extremely high resistance to wear in lubricated-friction conditions.

The equipment used to generate cavitation conditions is a standard piezoelectric crystal plates equipment, shown in fig. 2.3, from the Cavitation Laboratory [8], [9], [14], [35], [36], [42], [45], [87] within the Polytechnic University from Timisoara, whose operational parameters are constantly monitored and kept within the limits provided for in the ASTM G32-2010 standard, as follows:

- Vibration amplitude (double) = 50 µm
- Vibration frequency = 20 ± 0.02 kHz
- Power of the electronic ultrasound generator = 500 W
- Liquid environment = double-distilled water
- Liquid temperature = 22± 1°C

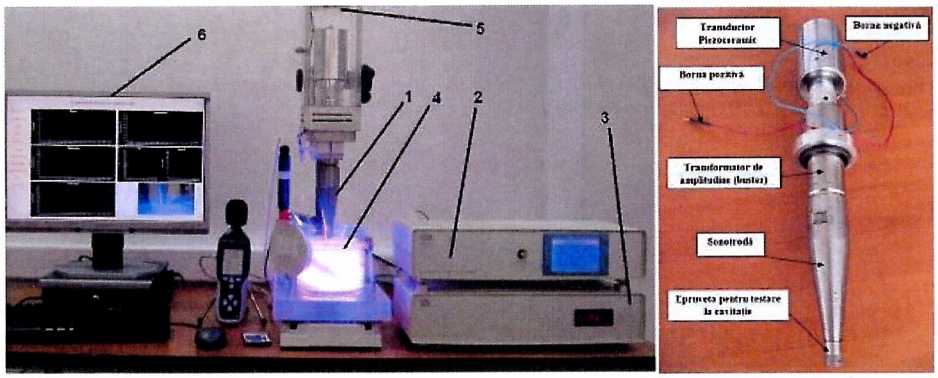

a) b)

Fig.2.3 The vibrator device with crystals piezoceramics

a) Image of the equipment used (1 - sonotrode; 2 - electronic system used to generate the vibration frequency and the power necessary for the 20 kHz/500 W piezoceramic

transducer; 3 - water temperature regulator; 4 - container for the liquid, with a serpentine cooler; 5 - piezoceramic transducer ventilation/cooling system; 6 - computer, used to command and control the vibratory device parameters).

b) Vibratory mechanic system

At the end of the 165 minutes of exposure to vibratory cavitation, the morphology of the sample structure, destroyed by cavitation erosion, is analyzed under the scanning electron microscope (TESCAN VEGA 3 LMU Bruker EDX Quantax, shown in fig. 2.11) which, by energy dispersive X-ray analysis (EDX), allows us to identify the proportions of the chemical elements existing in the tested samples, in relation to the nature of the structural components and the investigated area.

Fig.2.11 The scanning electron microscope TESCAN VEGA 3 LMU Bruker EDX Quantax

The macro- and micro-examinations, after the metallographic attack, are performed using the Olympus SYX7 microscope, shown in fig. 2.13, equipped with a series of eyepieces, objectives and lighting methods, allowing large zooming, according to the objective of the evaluation

Fig. 2.13 The OLYMPUS SYX7 microscope

The characteristics of the cavitation-eroded surface, expressed by the roughness

parameters Ra, Rz and Rt, were measured on three 120° axes, using the Mitutoyo SJ 210 analyzer, shown in fig. 2.14, at the offices of the company Inteliform S.R.L. from Timisoara

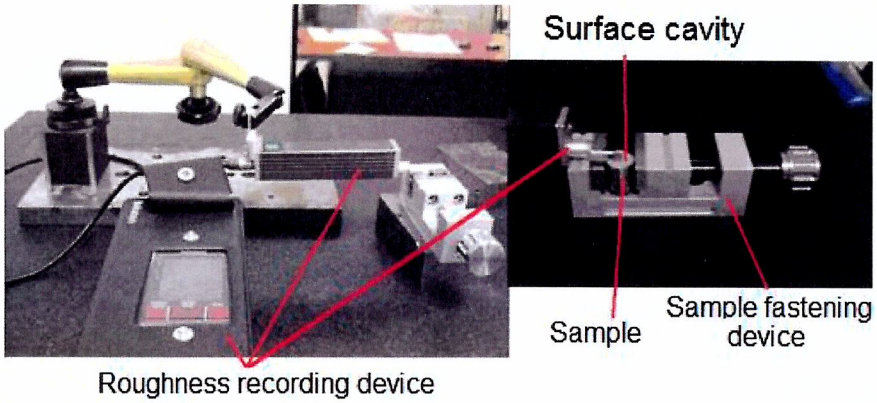

Fig.2.14. Roughness measurement on three axes, using the Mitutoyo SJ 210 digital analyzer.

The average/approximation curves of the values resulted from the experiment, at intermediary attack intervals, i.e. MDE(t) and MDER(t), are expressed as decided within the team lead by Mr. Bordeasu [87], [93]:

$$MDE\ (t) = A \cdot t \cdot (1 - e^{-B \cdot t})$$

$$MDER(t) = A \cdot (1 - e^{-B \cdot t}) + A \cdot B \cdot t \cdot e^{-B \cdot t} \quad (2.1)$$

where:

A - is the scale parameter, statistically determined and used for drawing the approximation curve, provided that the deviation of the experimental points from this curve is minimal

B - is the shape parameter of the curve

The experimental values, approximated by the two curves described by the expressions in (1), are calculated based on the mass losses m, recorded at the end of each intermediary test interval, "i", according to the expressions below.

$$MDE_i = \sum_{i=1}^{12} \left(\frac{4 \cdot \Delta m_i}{\rho \cdot \pi \cdot d_p^2}\right)$$

$$MDER_i = \frac{4 \cdot \Delta m_i}{\rho \cdot \pi \cdot d_p^2 \cdot \Delta t_i} \quad (2.2)$$

ρ - material density, in grams/mm^3,

Δti – duration of the cavitation, equal to the "i" interval (5 minutes, 10 minutes or 15 minutes)

d_p – the diameter of the sample surface subject to cavitation attack (d_p= 15,8 mm),

Conclusions

1.The copper-based alloys (bronze and brass), combined with fining chemical elements and using the appropriate treatment technologies, are able to modify their structure and mechanical properties, thus increasing the resistance to the erosion caused by cavitation bubbles formed mainly in hydropower equipment and not only.

2. The standard piezoelectric crystal assembly, available in the Cavitation Research Laboratory at the Polytechnic University from Timisoara, and used for cavitation testing, is a modern and highly efficient piece of equipment which, by allowing the setting of its operational parameters at the values indicated in the ASTM G32-2010 standard, offers the guarantee regarding research accuracy.

3. The microscopes available in the Materials Engineering Laboratory at the Polytechnic University from Timisoara, and used to analyze the structural changes, are modern and highly accurate, thus allowing us to perform the experiment according to the highest scientific requirements.

4. The methods used to study the behavior of samples to vibratory cavitation and to estimate their resistance comply with the ASTM G32-2010 standard and are commonly applied in the Cavitation Laboratory and in the Materials Engineering Laboratory at the Polytechnic University from Timisoara.

3. RESEARCH IN THE RESISTANCE TO VIBRATORY CAVITATION OF CuZn39Pb3 BRASS AND CuSn12-C BRONZE OF SEMI-FINISHED CONDITIONS

The tests regarding the behavior and resistance to cavitation erosion have been performed using the standard piezoelectric crystal assembly, available in the Cavitation Research Laboratory at the Polytechnic University from Timisoara, presented in Chapter 2.

The procedures for sample preparation before tests are performed, the total and intermediary duration of the vibratory cavitation attack intervals, the recording of the mass losses in relation to the cavitation intervals, as well as sample preservation, comply with the provisions in the ASTM G32-2010 standard and in the laboratory regulations.

3.1 Research in the resistance to cavitaton of CuZn39Pb3 brass

Diagrams 3.2 and 3.3 show the experimental values and the analytical approximation curves for the MDE and MDER parameters, which allow us to analyze the behavior of brass while being exposed to vibratory cavitation.

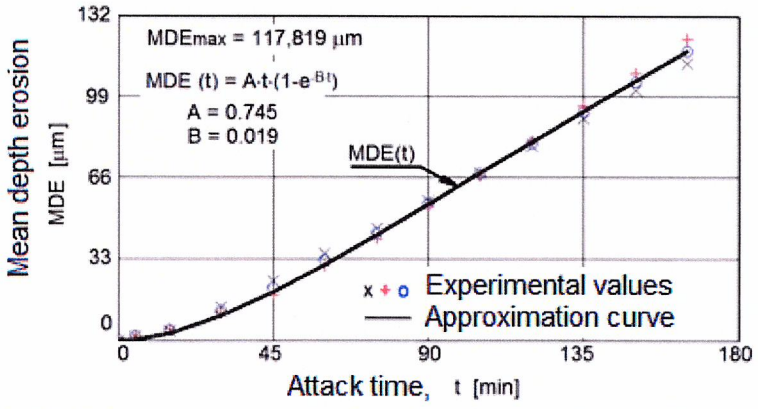

Fig.3.2 Evolution of mean depth erosion against cavitation exposure time

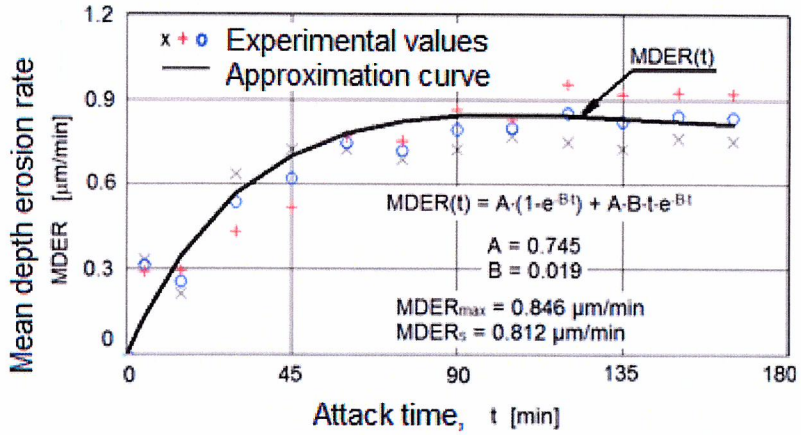

Fig.3.3 Evolution of mean depth erosion rate against cavitation exposure time

Fig. 3.6 only shows macroscopic images taken at the end of the test, for the three sets of tested samples, indicating an identical damage, but also proving that the tests were performed in identical conditions and under strict observance.

Min 0 Min 15 Min 90 Min 135 Min 165

Fig.3.5 Images of specimen surface at different cavitation exposure time (Sample 3)

Sample 1	Sample 2	Sample 3

Fig.3.6 Macroscopic images (taken with a Canon A480 camera) of the surfaces eroded by vibratory cavitation, after 165 minutes of cavitation exposure

The crevice size increases, and the crack propagation expands both at the surface and in depth, with cracks forming along the grain boundaries, as seen in the images in fig.3.7, taken using the scanning electron microscope, where it can be seen how the grain β′ is removed and how the cracks propagate.

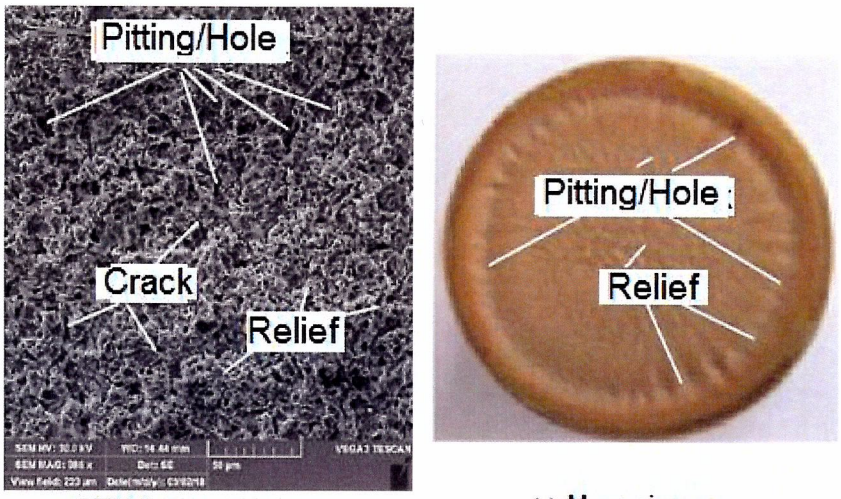

a) SEM limage (1000 x) b) Macro image

Fig.3.7 SEM and macroscopic images of the eroded microstructure, after a 165-minute exposure to cavitation
(the images are taken from the inferior area of the surface subject to cavitation)

Fig. 3.9 shows, as an example, the values of the three roughness parameters indicated on the screen, as well as the profile diagrams recorded on a 4-mm length, which better illustrate the crevices created in the material structure.

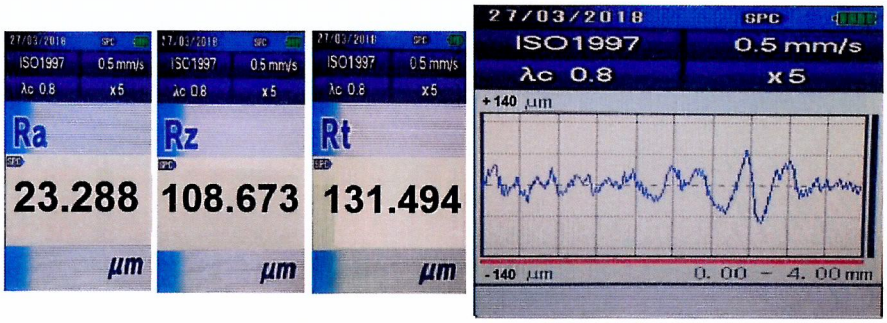

Min 165

Fig.3.9 Roughness parameters and profile registered with the Mitutoyo SJ 201 P device (Sample 3).

The morphologic analysis of the eroded structure was performed on the images obtained using the Vega 3 Tescan scanning electron microscope, available in the Materials Engineering Laboratory at the Polytechnic University from Timisoara.

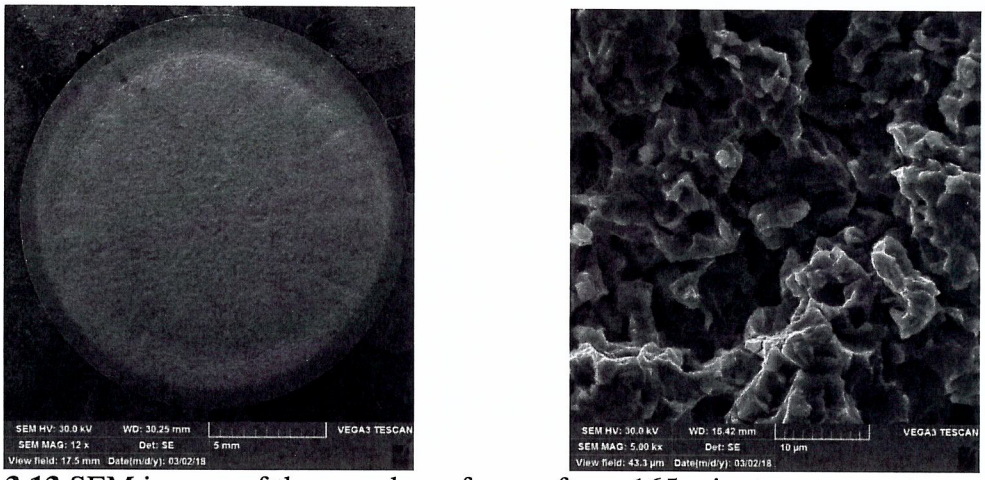

Fig. 3.13 SEM images of the sample surfaces, after a 165 minute exposure to cavitation.

The distinct characteristics of the cavitation-eroded sample surface are determined by a number of irregular crevices, resulted from the removal of the Cu-Zn compound (β′ - phase), i.e. increased toughness and brittleness.

Also, other crevices are caused by the Pb-inclusions inside solid-state solution α grains, resulted from the substitution of Zn with Cu.

3.2 Research in the resistance to cavitaton of CuSn12-C bronze

Fig. 3.14 and Fig. 3.15 present the specific diagrams using the experimental values, recorded on the three tested samples, for the cumulated average erosion depth (MDE), the average erosion penetration speed (MDER), and the approximation and mediation curves for these values, MDE(t) and MDER(t).

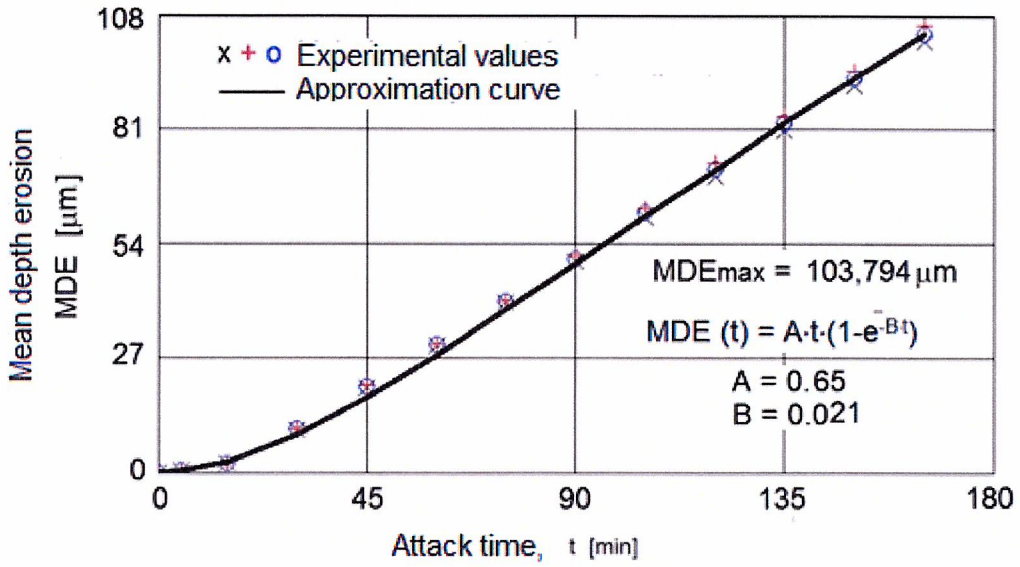

Fig.3.14 Evolution of mean depth erosion against cavitation exposure time

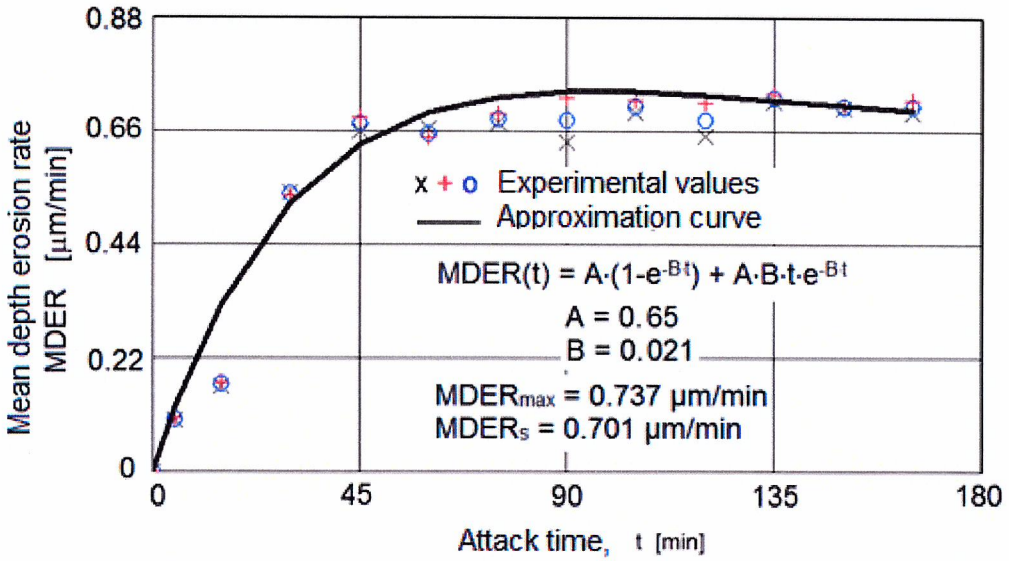

Fig.3.15 Evolution of mean depth erosion rate against cavitation exposure time

The way in which the surface structure is degraded, with the occurrence of cracks, pitting and crevices (slightly different from the way in which brass (CuZn39Pb3) is degraded), during the exposure to vibratory cavitation, is shown in the images taken with the Canon camera, from Fig. 3.17 and 3.18, as well as the image under the microscope, from Fig. 3.19.

Min 0 Min 15 Min 90 Min 135 Min 165

Fig.3. Images of specimen surface at different cavitation exposure time (Sample 2)

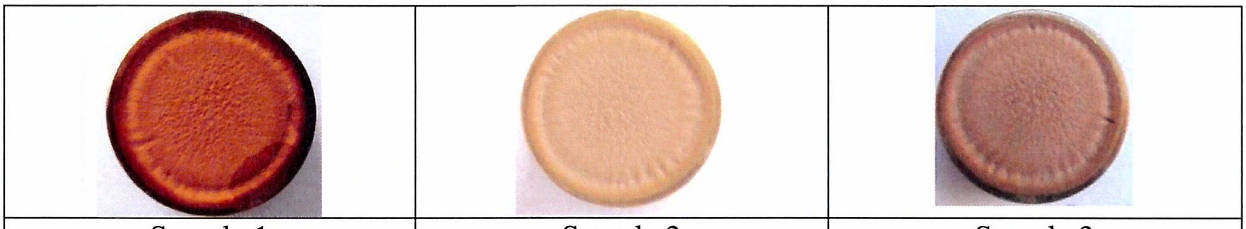

Sample 1	Sample 2	Sample 3

Fig.3. Macroscopic images (taken with a Canon A480 camera) of the surfaces eroded by vibratory cavitation, after 165 minutes of cavitation exposure

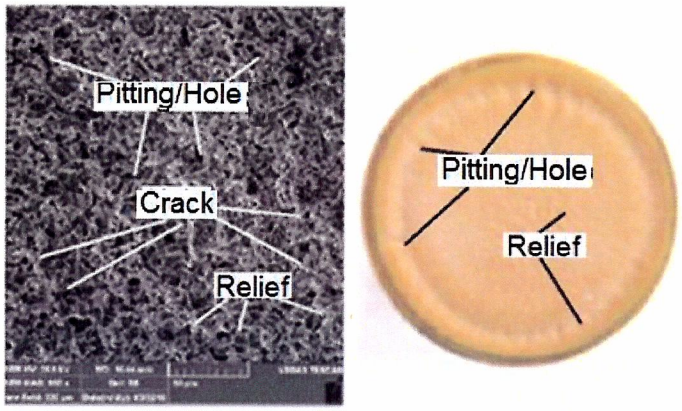

a) SEM image b) Macro image

Fig.3.19 SEM and macroscopic images of the eroded microstructure, after a 165 minute exposure to cavitation

Fig. 3.20 shows roughness profiles, using the values of the parameters Ra, Rz şi Rt, obtained through measurements performed with the Mitutoyo SJ 210 P digital analyzer, at the four moments deemed as suggestive for the way in which samples behave when subject to vibratory cavitation.

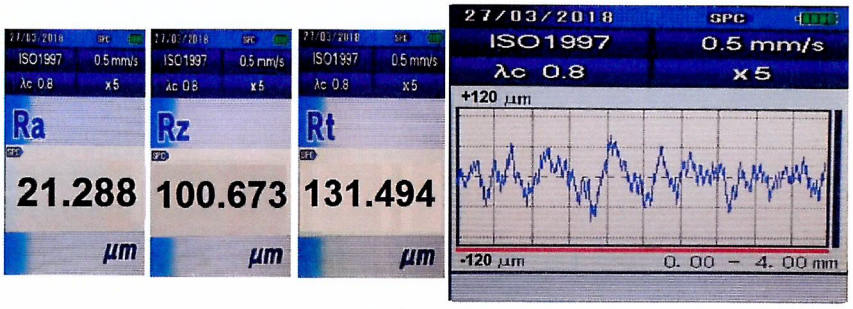

Min 165

Fig.3.20 9 Roughness parameters and profile registered with the Mitutoyo SJ 201 P device (Sample 2)

The SEM investigation of the bronze sample surface subject to cavitation erosion (fig. 3.24) reveals the formation of evenly distributed pitting in the matrix of solid solution α, which substitutes SN in Cu, and the occurrence of polyhedral indentations in the areas with the electronic compound δ, characterized by increased brittleness.

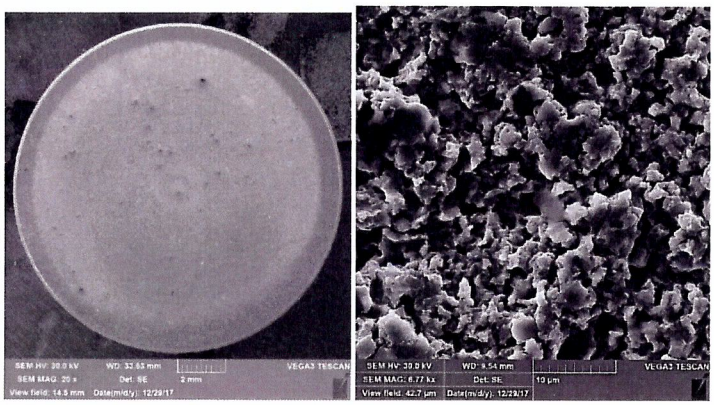

-a- **-b-**

Fig.3.24 SEM images of the sample surfaces, after a 165 minute exposure to cavitation.

3.3 Comparison of the research results

The curves and parameter values illustrated in diagrams in figures 3.25 and 3.26 show the differences and similarities between the behaviors and resistances to cavitation of the two materials presented in this chapter.

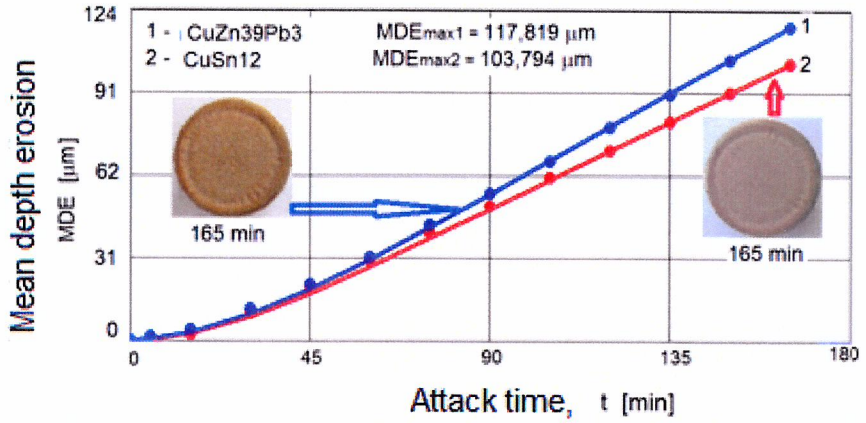

Fig.3.25 Comparisons of the cavitation erosion behavior taking into account the mean depth erosion

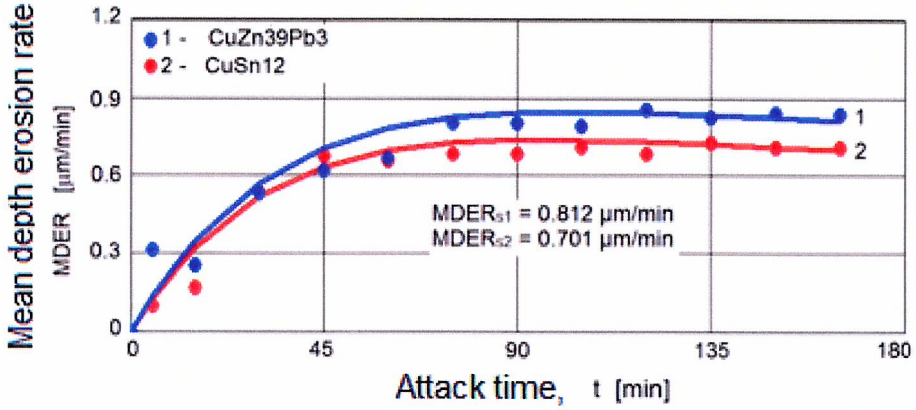

Fig.3.26 Comparisons of the cavitation erosion behavior taking into account the mean depth erosion rate

Similarities:

- similar exponential evolution of the MDE(t) curves, with a plateau starting with minute 45;
- similar evolution of the MDER(t) curves, which reach maximum values after 90 minutes of cavitation erosion-corrosion attack;
- approximately identical dispersions of the experimental values and their arithmetic averages for the three samples, in comparison with the mediation curves MDER(t), starting with minute 45 of the exposure to cavitation;

The differences result from a better behavior of bronze (CuSn12), as shown in the bar chart from fig. 3.27, which compares the erosion parameters (cumulated average erosion depth, after 165 minutes of cavitation errosion-corrosion attack, MDEmax and the cavitation resistance, Rcav = 1/MDERs) and also by comparing the values of the roughness parameter Rz

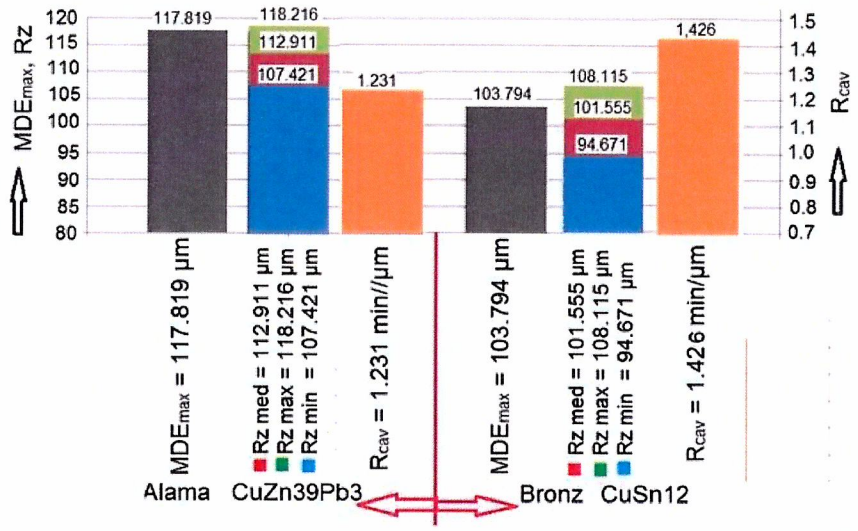

Fig.3.27 Bar chart estimating the resistance to cavitation erosion-corrosion, by comparing the values of the specific parameters

3.4 Conclusions

1. Brass (CuZn39Pb3) and bronze (CuSn12-C) display the behavior specific to materials with evenly distributed structural components; however, they have low mechanical resistance, therefore the materials in their initial research state (as delivered) can only be used for parts operating in low-cavitation hydrodynamic conditions, i.e. hydraulic equipment (pressure valves, speed and flow regulators, thread valves, etc.), which operate with fluids with a higher viscosity than water.
2. The start and advancement of the damage under the impingement of microjets and shock waves developed in the cavitational process, occur at the boundary between the solid solution α and the electron component β' with a rapid destruction of phase β' - in the case of brass -, and at the boundary between the solid α and the electron component δ, expanding in the solid solution α.
3. Both materials show similar behaviors to cavitation erosion-corrosion, yet they display slightly different resistances (with an approx. 11% increase for bronze CuSn12-C).
4. The two materials (i.e. brass CuZn39Pb3 and bronze CuSn12-C) can be used in producing the parts operating in increased cavitation hydrodynamic systems, such as ship propellers and/or hydraulic equipment impellers, only if those parts go through in-depth heat treatment.

4. RESEARCH INTO THE RESISTANCE TO CAVITATON OF CERTAIN COPPER-BASED ALLOYS SUBJECT TO IN-DEPTH HEAT TREATMENT

In-depth heat treatments are required in order to obtain certain physical and mechanical properties and to modify the structure of the material, by varying the temperatures, the tempering duration and the cooling environment/speed [23].

4.1 Research in the resistance to cavitaton of CuZn39Pb3 brass

4.1.1 In-depth heat treatment

The diagram in fig. 4.1 shows the cycle of the 4 types of heat treatment:
- Hardening at 800°C (maintained for 40 minutes. followed by cooling in water) – marked as **C 800**;
- Hardening at 800°C (maintained for 40 minutes. followed by cooling in water), then tempering at 250°C (maintained for 60 minutes, followed by cooling at ambient temperature – marked as **C 800/R 250**;
- Hardening at 800°C (maintained for 40 minutes. followed by cooling in water), then tempering at 400°C (maintained for 60 minutes, followed by cooling at ambient temperature) – marked as **C 800/R 400**;
- Hardening at 800°C (maintained for 40 minutes. followed by cooling in water), then tempering at 600°C (maintained for 60 minutes, followed by cooling at ambient temperature)– marked as **C 800/R 600).**

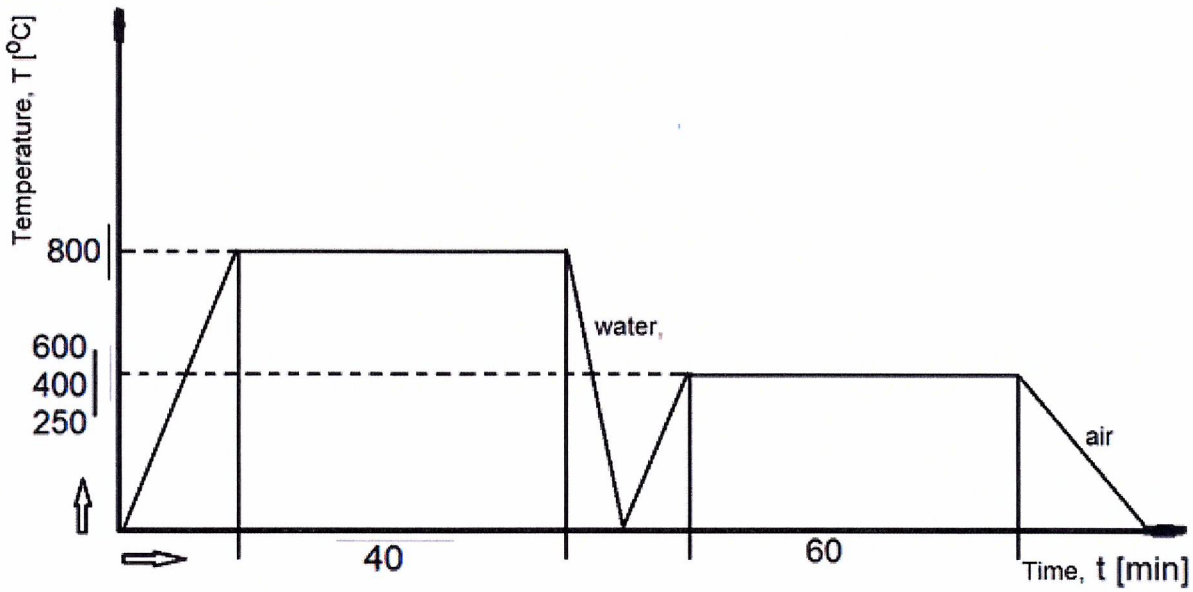

Fig.4 Diagram of volume heat treatments

4.1.2 Results of cavitation analysis

In-depth hardening starting with 800°C

The experimental values obtained from the cavitation test, as recorded during the vibratory cavitation tests, as well as the mediation curves MDE(t) and MDER(t), are shown in figures 4.2 and 4.3.

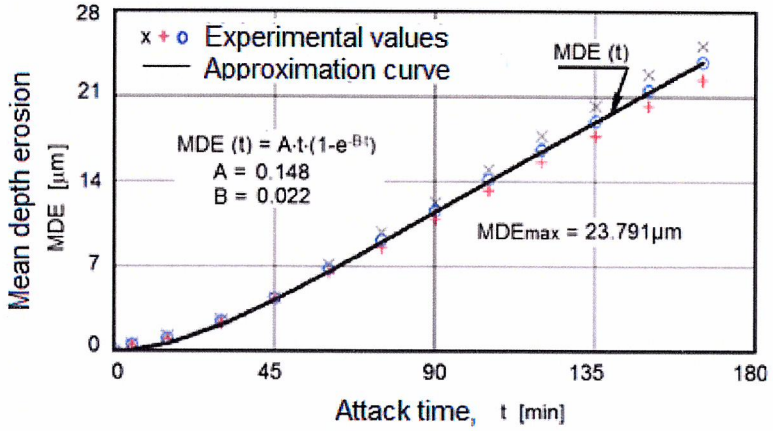

Fig. 4.2 Evolution of mean depth erosion against cavitation exposure time

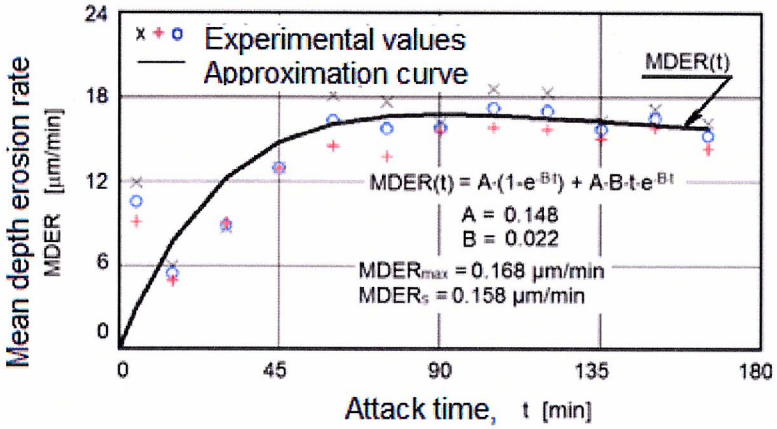

Fig.4.3 Evolution of mean depth erosion rate against cavitation exposure time

Fig. 4.5 shows images of the evolution of erosion in the area of the sample surface exposed to cavitation, in terms of expansion and depth, for a randomnly-chosen sample, identified during the tests as Sample 1.

Fig. 4.6 shows images of the degraded surfaces in the three tested samples, after the cavitation test has ended (165 minutes).

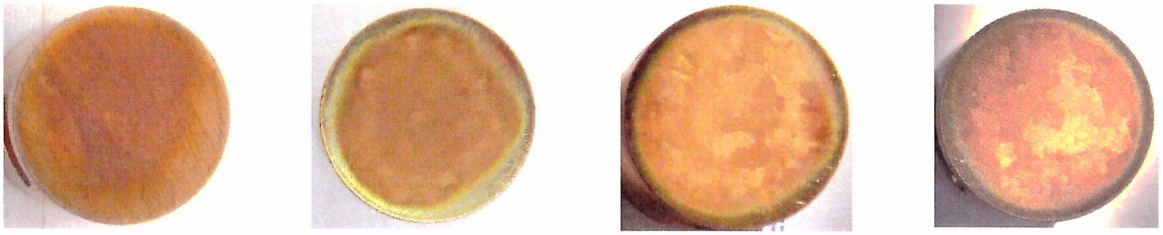

Min 15 Min 90 Min 135 Min 165

Fig.4.5 Images of specimen surface at different cavitation exposure time (Sample 1)

Sample 1 Sample 2 Sample 3

Fig.4.6 Macroscopic images (taken with a Canon A480 camera) of the surfaces eroded by vibratory cavitation, after 165 minutes of cavitation exposure

The porous appearance of the sample surface, with cracks, reliefs and crevices, is shown in the SEM and macroscopic images from fig. 4.7, as recorded on one of the three samples, at the end of the corrosion-erosion test.

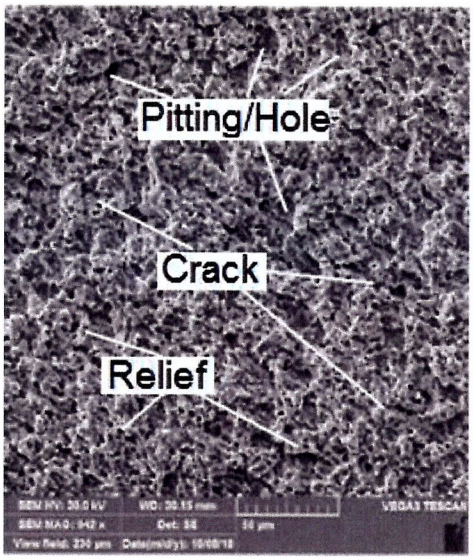

a) Imagine SEM (1000 x)

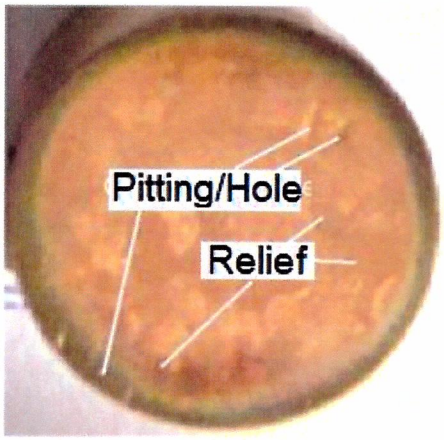

b) Imagine macro

Fig.4.7 SEM and macroscopic images of the eroded microstructure, after a 165 minute exposure to cavitation (**Sample 2**)

Fig. 4.8 shows the profile diagram with the values of the three reference parameters (R_a, R_z si R_t), as recorded with the Mitutoyo SJ 201 analyzer.

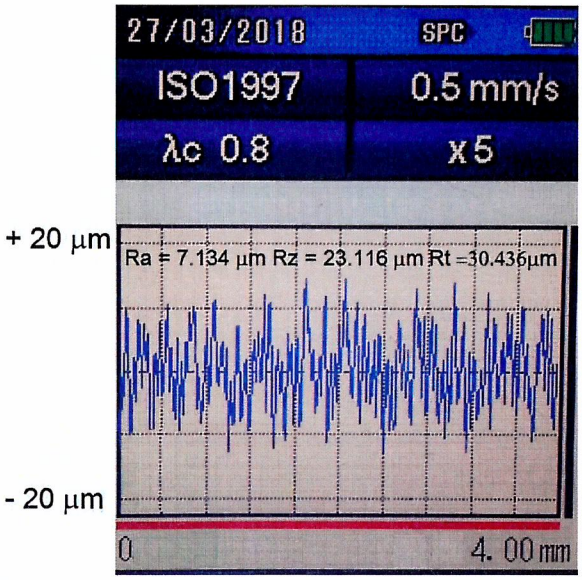

Fig.4.8 Roughness parameters and profile registered with the Mitutoyo SJ 201 P device (**Sample 1**)

The relief of the sample, after the cavitation-erosion test, for 165 minutes (fig. 4.10 a, b) shows an evenly degraded surface, with small ductile tearing indentations.

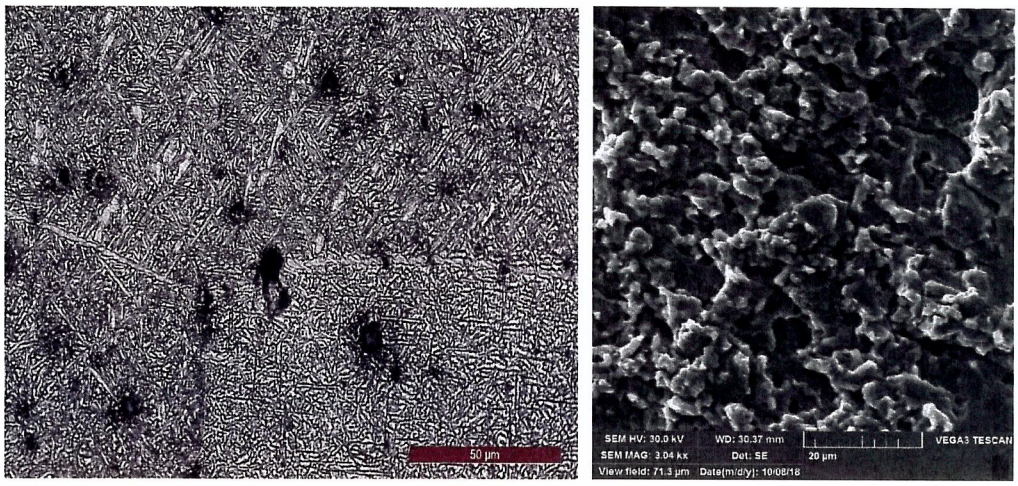

-a- -b-

Fig.4. Macroscopic image (a) and SEM image SEM (b), after a 165 minute exposure to cavitation

In-depth hardening starting at 800°C, with tempering at 250 °C

Figures 4.11 and 4.12 show the experimental values for the three tested samples, as approximated by the mediation curves MDE(t) and MDER(t), generated based on the analytical formulas from (2.1), as well as by the values of the parameters MDE_{max}, $MDER_{max}$ and $MDER_s$.

The statistical processing of the experimental data obtained for the three samples, with a 0.253 standard deviation and a frequency band within a 99% tolerance, shows that the entire research process, carried out on the three samples, has been performed in identical and accurate conditions.

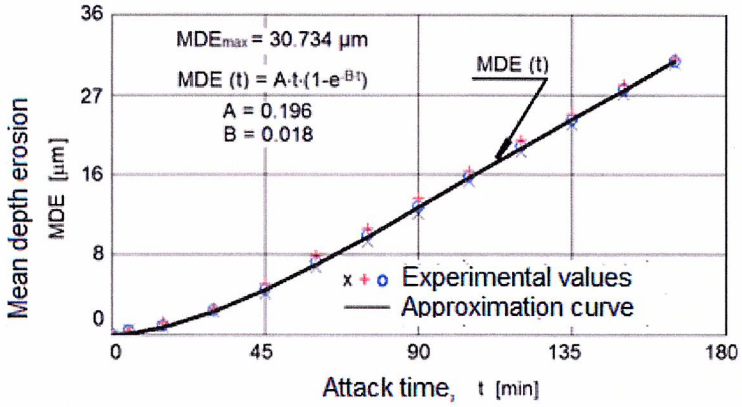

Fig. 4.11 Evolution of mean depth erosion against cavitation exposure time

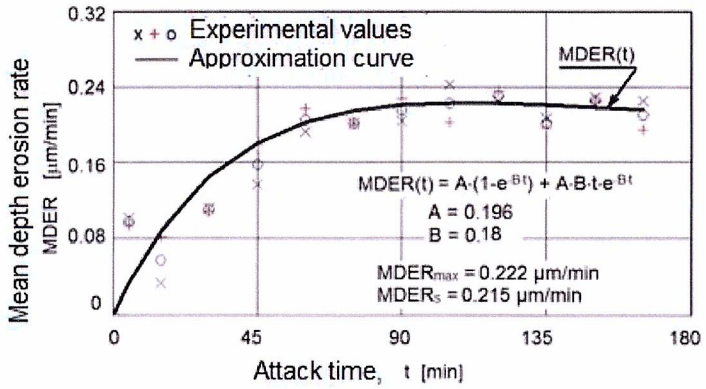

Fig. 4.12 Evolution of mean depth erosion rate against cavitation exposure time

Fig. 4.14 and 4.15 show photographic, macroscopic images, indicating the evolution of the cavitation-erosion in the areas of the exposed surface, at various intervals and after 165 minutes.

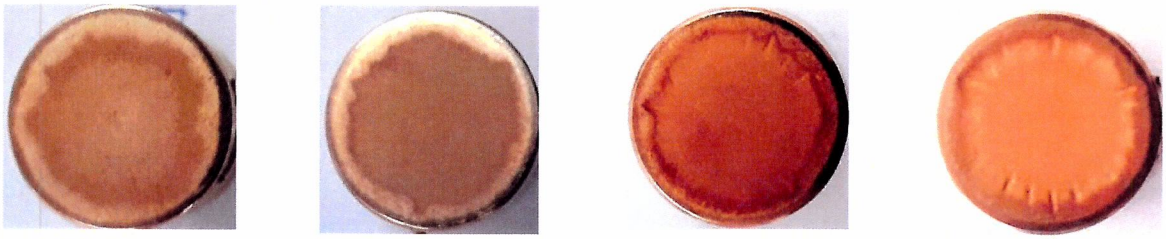

Min 15 Min 105 Min 135 Min 165

Fig.4.14 Images of specimen surface at different cavitation exposure time (Sample 3)

Sample 1 Sample 2 Sample 3

Fig.4.15 Macroscopic images (taken with a Canon A480 camera) of the surfaces eroded by vibratory cavitation, after 165 minutes of cavitation exposure

The SEM image in fig. 4.16 shows the nature of the structure, more homogeneous and fine, as a result of the 800°C-heat treatment, followed by a tempering at 250°C, as well as the networks of cracks and pitting, also indicated in the macroscopic image from fig. 4.16 b.

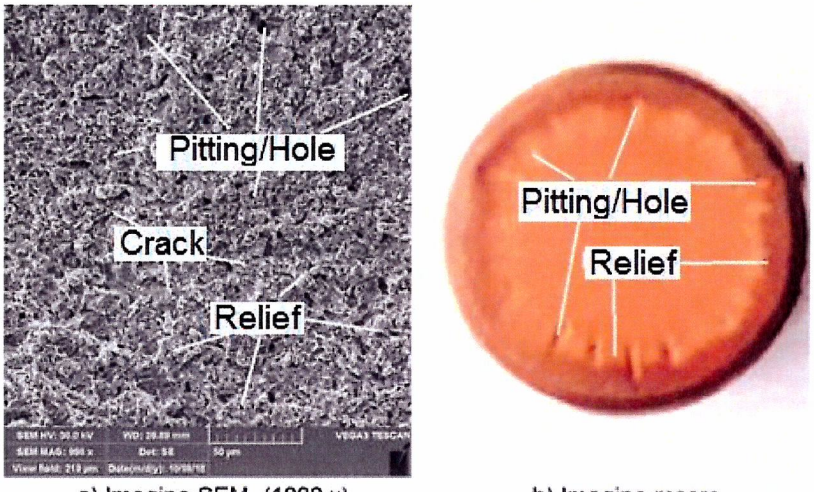

a) Imagine SEM (1000 x) b) Imagine macro

Fig. 4.16 SEM and macroscopic images of the eroded microstructure, after a 165 minute exposure to cavitation (**Sample 3**)

Fig. 4.17 shows the profile diagram of a segment from the eroded surface, with the values for the three roughness parameters.

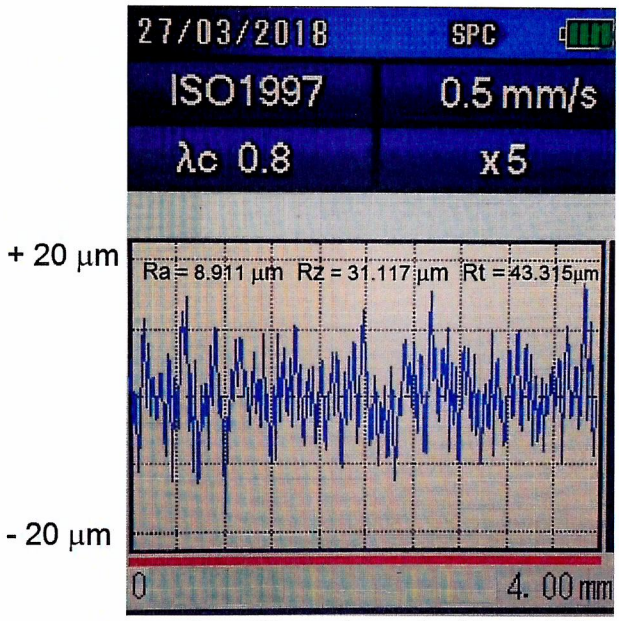

Fig.4.17 Roughness parameters and profile registered with the Mitutoyo SJ 201 P device **(Sample 3)**

After the tempering heat treatment is applied at 250°C, certain acicular α-phase particles precipitate from the over-saturated β-phase, both inside the grains and at the grain boundary (fig. 4.19 a), the internal tensions are lowered and the indentations resulted from the cavitation attack are more obvious in the grain-boundary area. (fig. 4.19 b).

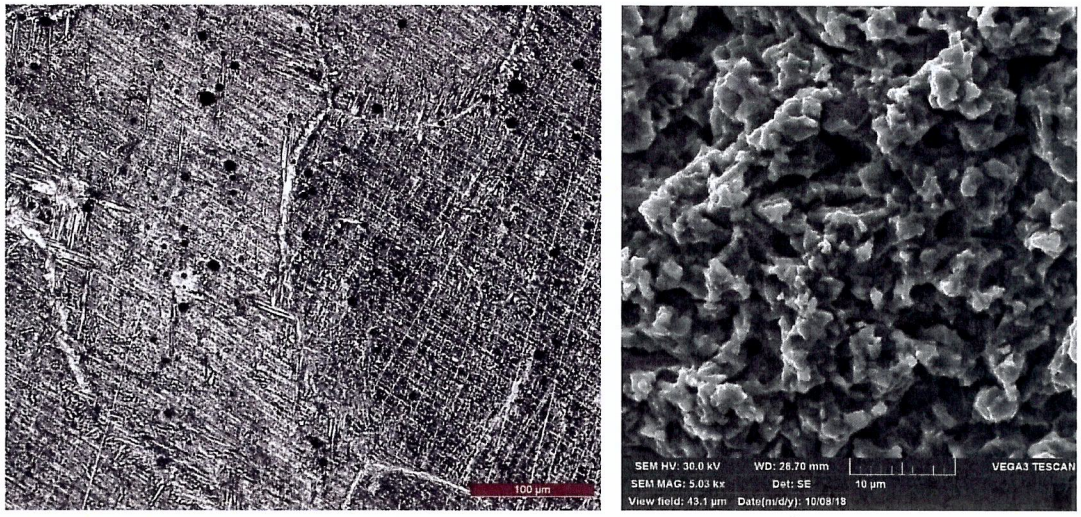

-a- **-b-**

Fig.4.19 Macroscopic image (a) and SEM image SEM (b), after a 165 minute exposure to cavitation

In-depth hardening starting at 800°C, with tempering at 400 °C

Figures 4.20 and 4.21 show the results of the cavitation-erosion test, as experimental values for the three tested samples, as approximated by the mediation curves MDE(t) and MDER(t), as well as by the values of the parameters MDE_{max}, $MDER_{max}$ and $MDER_s$.

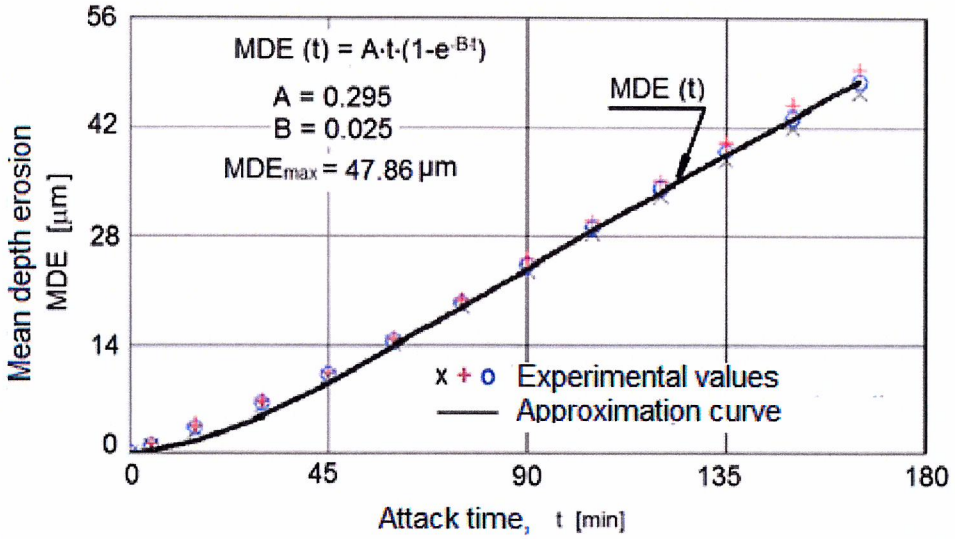

Fig.4.20 Evolution of mean depth erosion against cavitation exposure time

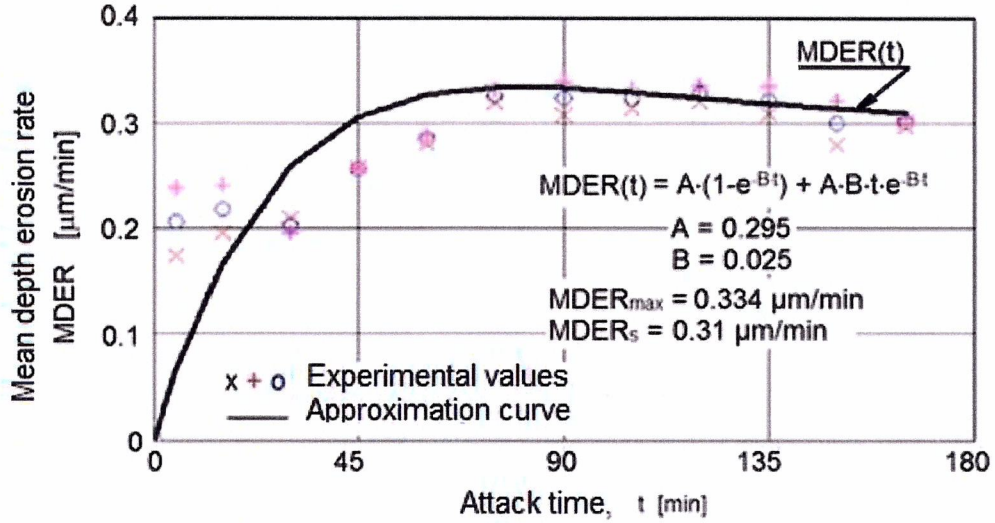

Fig.4.21 Evolution of mean depth erosion rate against cavitation exposure time

Fig. 4.23 shows images with the evolution of erosion, as the sample is exposed to cavitation erosion-corrosion, while fig. 4.24 shows images of the eroded sample surfaces, after the cavitation test has ended.

The SEM and macroscopic images from fig. 4.25 indicate the degree of surface damage, with a large number of crevices and cracks.

Min 15 Min 75 Min 135 Min 165

Fig.4.23 Images of specimen surface at different cavitation exposure time (Sample 2)

Sample 1 Sample 2 Sample 3

Fig.4.24 Macroscopic images (taken with a Canon A480 camera) of the surfaces eroded by vibratory cavitation, after 165 minutes of cavitation exposure

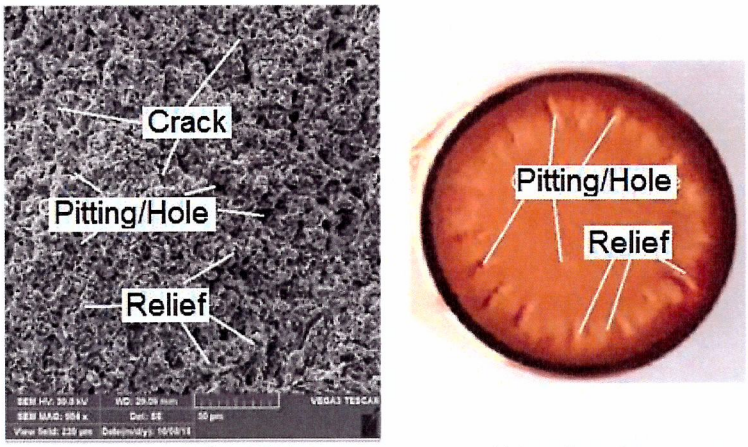

a) Imagine SEM (1000 x) b) Imagine macro

Fig.4.25 SEM and macroscopic images of the eroded microstructure, after a 165 minute exposure to cavitation (**Sample 2**)

The profile diagram from fig. 4.26 shows, with significant differences in the values for the roughness parameter, recorded for Sample 3, the evolution and the structural deterioration of the material subject to in-depth hardening at 800°C, with tempering at 400°C, in the exposed area.

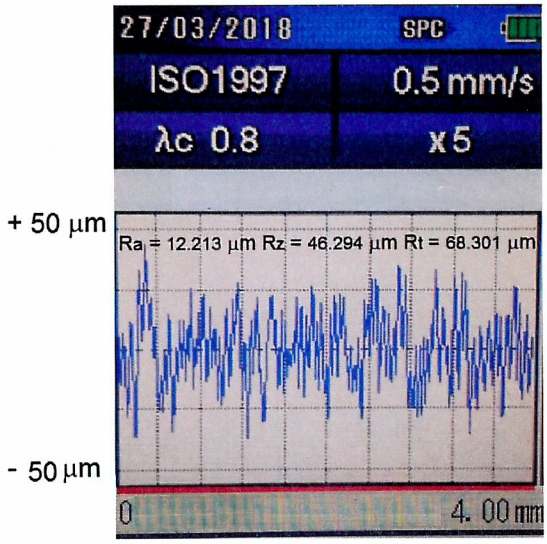

Fig.4.26 Roughness parameters and profile registered with the Mitutoyo SJ 201 P device **(Sample 3)**

The increase in the tempering temperature to 400°C results in an acceleration of the precipitation process of phase α from phase β, as well as an acceleration of the coalescence process of these particles, especially within the grain-boundaries (fig. 4.28 a), thus increasing the number of crevices occurring on the surface of the sample exposed to the cavitation-erosion test (fig. 4.18 b).

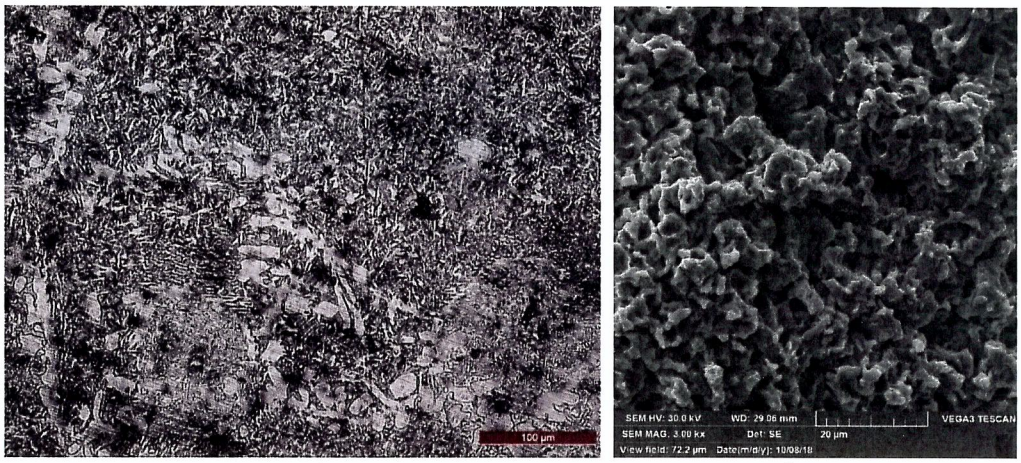

-a- -b-

Fig.4.28 Macroscopic image (a) and SEM image SEM (b), after a 165 minute exposure to cavitation

In-depth hardening starting at 800°C, with tempering at 600 °C

Fig. 4.29 and 4.30 show the results recorded during the cavitation-erosion tests performed on the three samples. These are expressed as experimental values and as mediation curves MDE(t) and MDER(t).

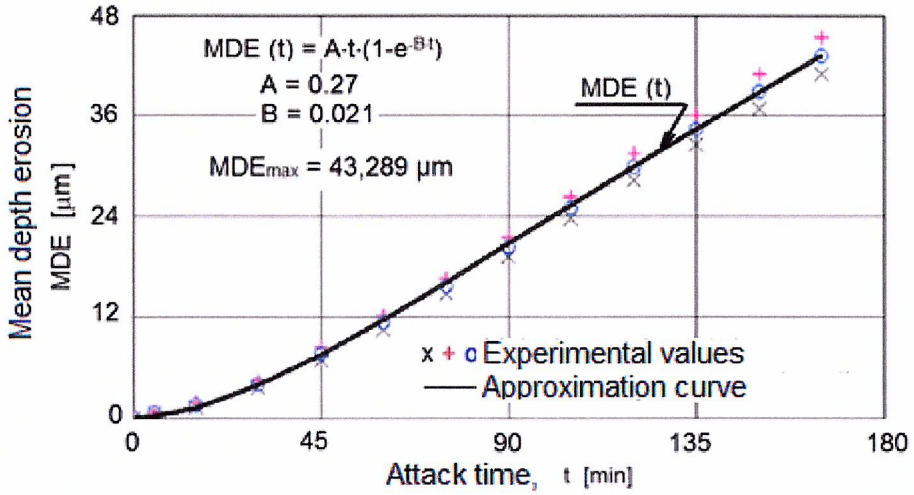

Fig.4.29 Evolution of mean depth erosion against cavitation exposure time

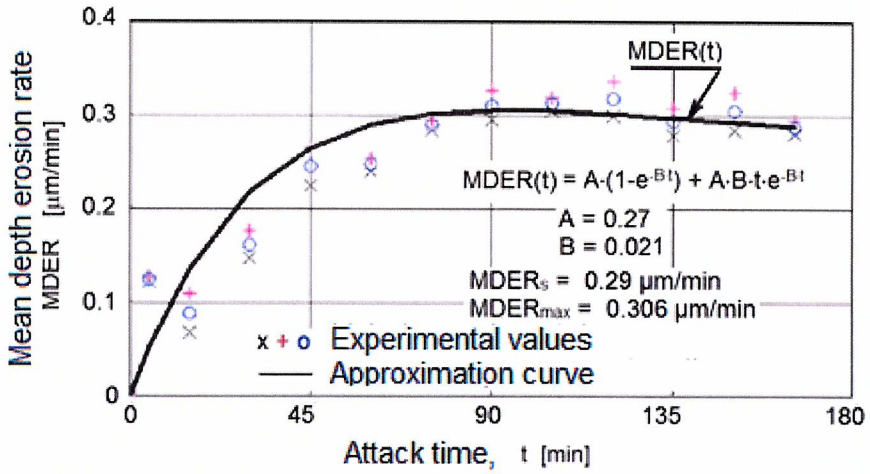

Fig.4.30 Evolution of mean depth erosion rate against cavitation exposure time

The effect of the heat treatment - hardening at 800°C and tempering at 600°C - on the behavior and of brass (CuZn39Pb3) to cavitation erosion, is also shown by the evolution of wear in the exposed areas of the three samples, as seen in the photographic images from fig. 4.32 and in the SEM image from fig .4.34.

The SEM image from fig .4.34a shows the crack and tearing propagation, with the formation of crevices, as a result of the impact between the structure and the microjets generated by the cavitation bubble implosion.

Min 15 Min 90 Min 135 Min 165

Fig.4.32 Images of specimen surface at different cavitation exposure time (Sample 1)

Sample 1 Sample 2 sample 3

Fig.4.33 Macroscopic images (taken with a Canon A480 camera) of the surfaces eroded by vibratory cavitation, after 165 minutes of cavitation exposure

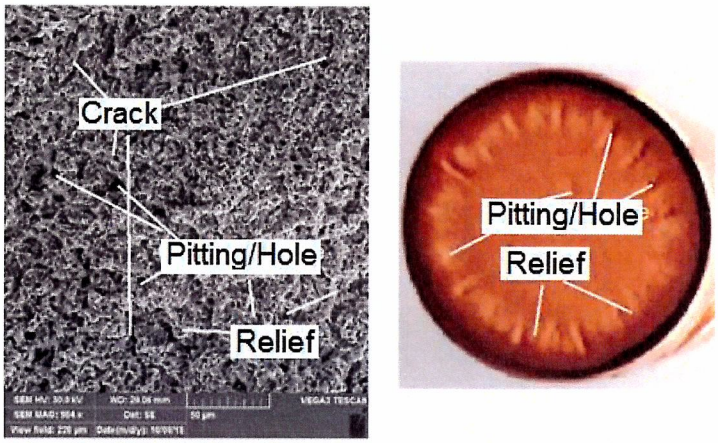

a) Imagine SEM (1000 x) b) Imagine macro

Fig.4.34 SEM and macroscopic images of the eroded microstructure, after a 165 minute exposure to cavitation (**Sample 1**)

The shape of the profile diagram from fig. 4.35, with significant differences in the values for the roughness parameters, shows that, unlike the previously applied heat treatments, the hardening at 800°C, with tempering at 600°C, applied in this case, has no significant effect on the surface material, with regard to the even resistance, in all contact points, to the cavitation microjets.

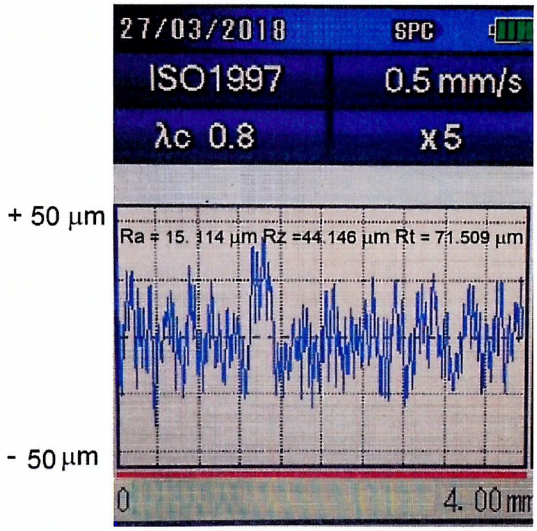

Fig.4.35 Roughness parameters and profile registered with the Mitutoyo SJ 201 P device (**Sample 1**)

The tempering at 600°C results in two other processes, occurring in parallel: on the one hand, we notice an increase in the α-phase precipitation into β-phase, causing a slight decrease in the amount of α-phase grains and, on the other hand, a more intense coalescence of the small acicular α-phase grains, which form larger, polygonal grains (Fig. 4.37 a).

The images showing the relief of the surface subject to cavitation-erosion (fig. 4.37 b) are fully in line with the previous results.

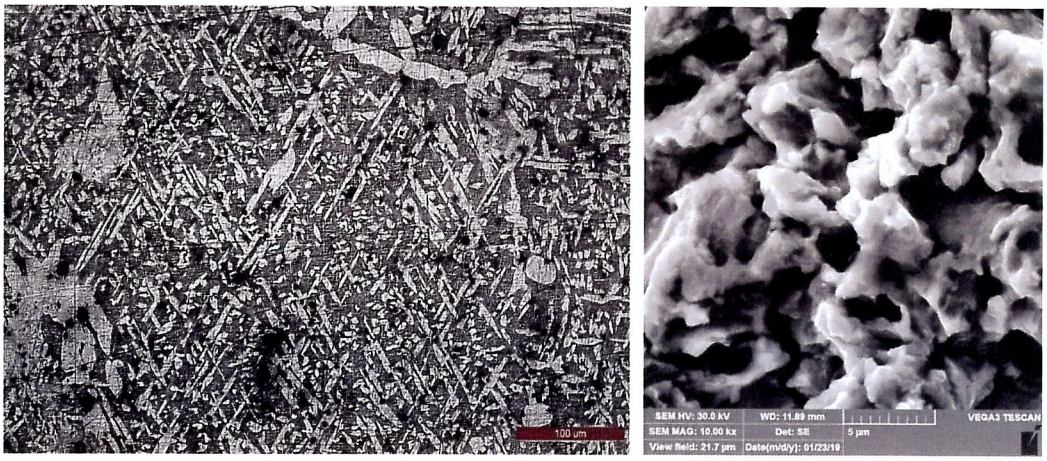

-a- -b-

Fig.4.37 Macroscopic image (a) and SEM image SEM (b), after a 165 minute exposure to cavitation

4.1.3. Comparison of the research results

The bar chart from fig. 4.42 shows the resistance resulted from the four heat treatment cycles, by comparing the values of the two reference parameters, i.e. R_{cav} and MDE_{max}, with the parameters of the control materials, i.e. OH12NDL and CuNiAl I-RNR, available in the Cavitation Research Laboratory at the Polytechnic University from Timisoara.

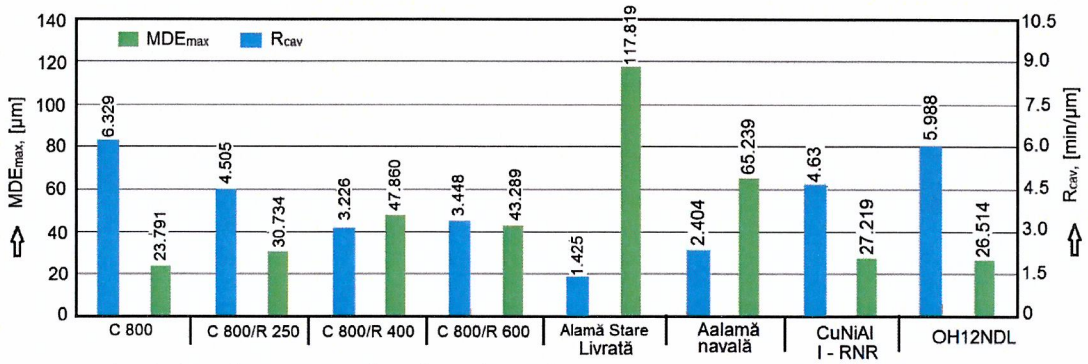

Fig.4.42 Histogram of estimation of resistance to erosion of cavitation (comparison of the heat treatment regimes and the standard materials)

The bar chart data show that, after hardening, the resistance of brass (CuZn39Pb3) exceeds the resistance of the control materials. According to the data from table 4.3, the maximum erosion depth decreases by 11.45% when compared with steel (OH12NDL), by 14.41% when compared with bronze (CuNiAl I-RNR), and by 174.22 % when compared with the brass used in the naval industry. Based on the values acquired by the R_{cav} parameter, we have noticed that the resistance to cavitation erosion increases by 5.7% when compared with stainless steel (OH12NDL), by 36.71% when compared with bronze (CuNiAl I-RNR), and by 163.29% when compared with the resistance of the brass used in the naval industry.

4.2Research in the resistance to cavitaton of CuSn12-C bronze

4.2.1 In-depth heat treatment

The diagram in fig. 4.43 shows the cycle of the 3 types of heat treatment:

- hardening at 700°C (maintained for 60 minutes. followed by cooling in water) – marked as **C 700**;
- hardening at 700°C (maintained for 60 minutes. followed by cooling in water), followed by

tempering at 250°C (maintained for 60 minutes. followed by cooling in ambient temperature - marked as **C 700/R 250**;
- hardening at 700°C (maintained for 60 minutes, followed by cooling in water), followed by tempering at 500°C (maintained for 60 minutes, followed by cooling in ambient temperature) - marked as **C 800/R 500.**

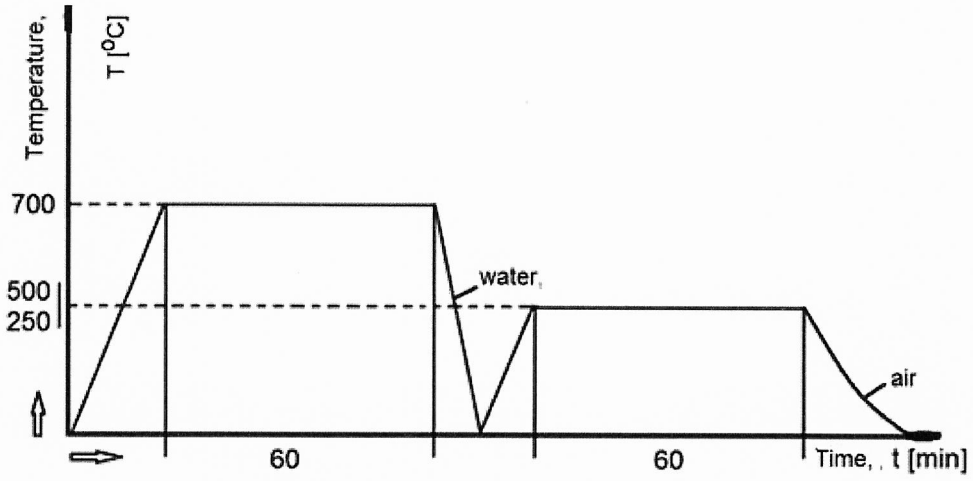

Fig.4.43 Diagram of volume heat treatments

4.2.2 Results of cavitation analysis

In-depth hardening starting with 700°C

The results of the cavitation-erosion tests, performed on the three samples, are shown for each of the 12 testing cycles and using the approximation/mediation curves, i.e MDE(t) from fig. 4.44, and MDER(t) from fig. 4.45, respectively.

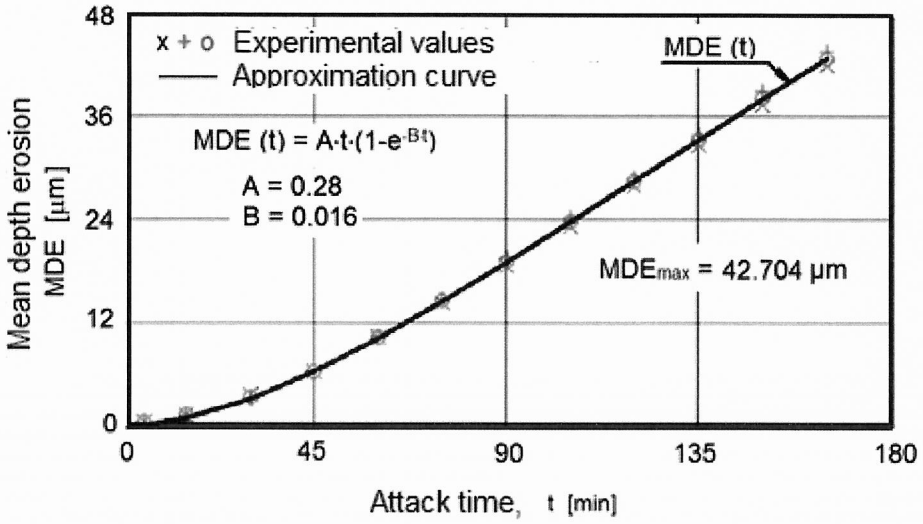

Fig.4.44 Evolution of mean depth erosion against cavitation exposure time

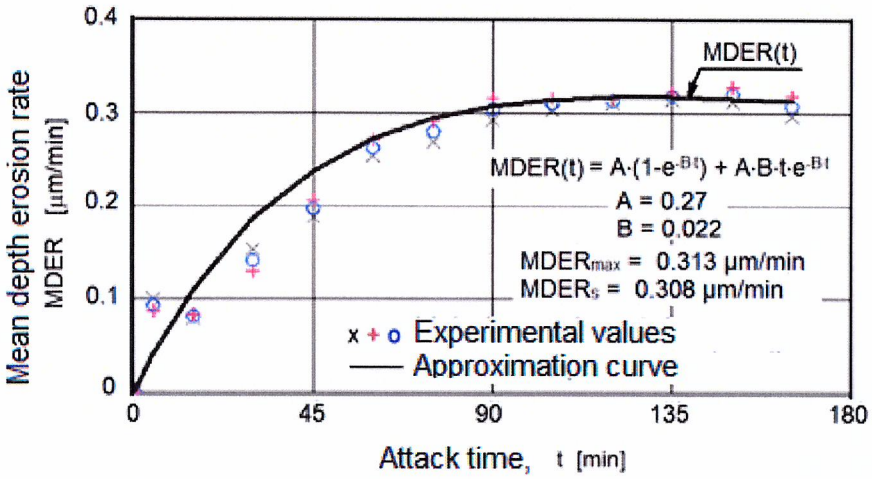

Fig.4.45 Evolution of mean depth erosion rate against cavitation exposure time

Figures 4.47 and 4.48 show photographic images of how erosion has expanded within the area of the exposed surface.

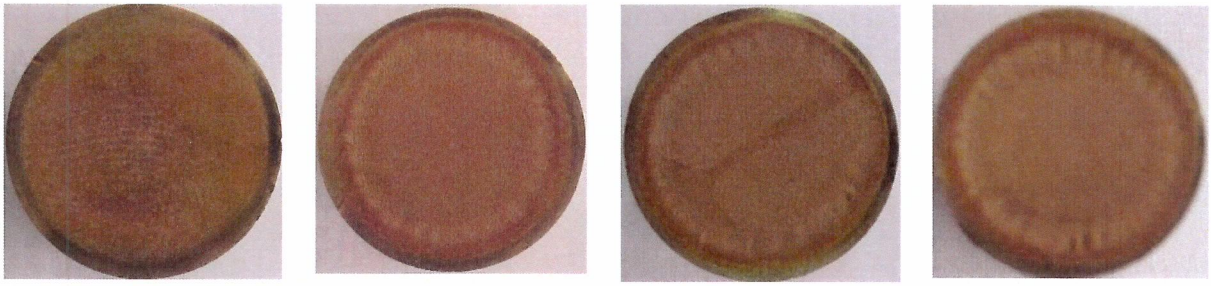

Min 15 Min 120 Min 135 Min 165

Fig.4.47 Images of specimen surface at different cavitation exposure time (Sample 3)

Sample 1 **Sample 2** **Sample 3**

Fig.4.48 Macroscopic images (taken with a Canon A480 camera) of the surfaces eroded by vibratory cavitation, after 165 minutes of cavitation exposure

The SEM image from fig. 4.49, correlated with the adjacent macroscopic image, shows the cracks, pitting and cavities created due to grain expulsion. These show how the erosion penetrates the structure of the material under the impact pressure caused by the cavitation microjets.

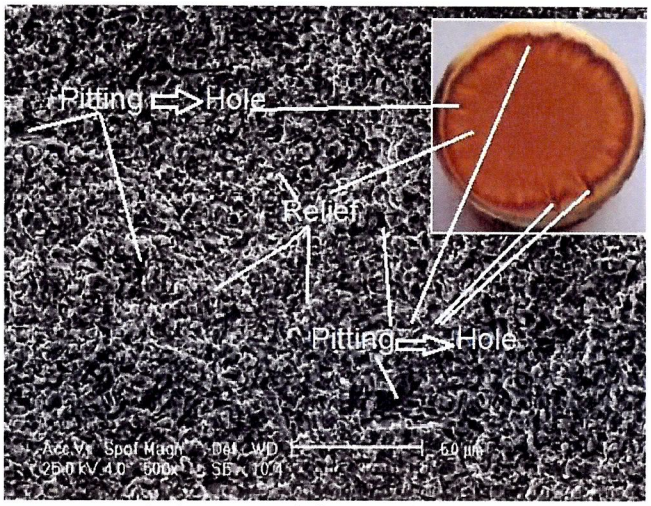

Fig.4.49 SEM and macroscopic images of the eroded microstructure, after a 165 minute exposure to cavitation – **Sample 1**

Fig. 4.50 exhibits an arbitrarily chosen bar chart, recorded for one of the three samples (identified as Sample 3), using the Mitutoyo analyzer, in order to determine the values for the roughness parameters (R_a, R_z and R_t).

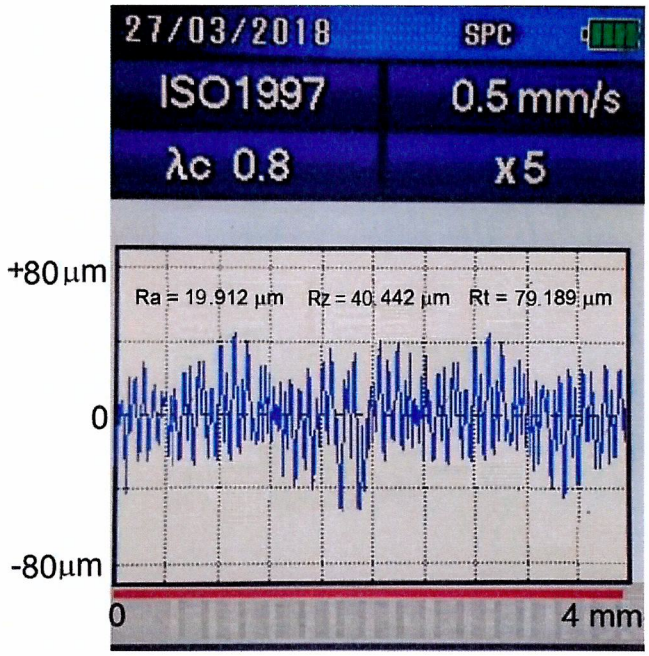

Fig. 4.50 Roughness parameters and profile registered with the Mitutoyo SJ 201 P device **(Sample 3)**

Prin hardening în apă până la temperatura camerei, fenomenele de difuzie fiind estompate, faza β devine suprasaturată, cu aspect apropiat de cel al martensitei din oţeluri, iar faza α nu suferă transformări (fig. 4.52 a).. Investigarea la microscopul electronic a suprafeţei erodate prin cavitaţie (fig.4.52 b) arată că ruperea are un caracter ductil, iar limitele dintre grăunţii de soluţie solidă α (fază mai moale şi plastică) reprezintă microzonele de initiere şi dezvoltare ulterioară a cavernelor de cavitaţie.

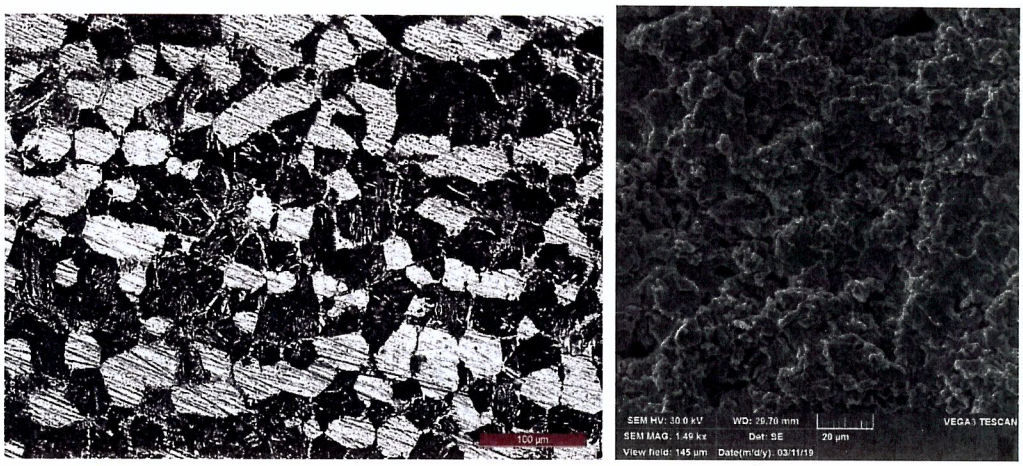

-a -b-

Fig.4.52 Macroscopic image (a) and SEM image SEM (b), after a 165 minute exposure to cavitation

In-depth hardening starting at 700°C, with tempering at 250 °C

Fig. 4.53 exhibits the experimental values of the cumulated mean depths, recorded on the three samples subject to cavitation-erosion tests, as well as their mediation curve MDE(t).

Fig. 4.54 exhibits the experimental values of the mean depth of penetration rates, recorded on the three samples subject to cavitation-erosion tests, as well as their mediation curve MDE(t).

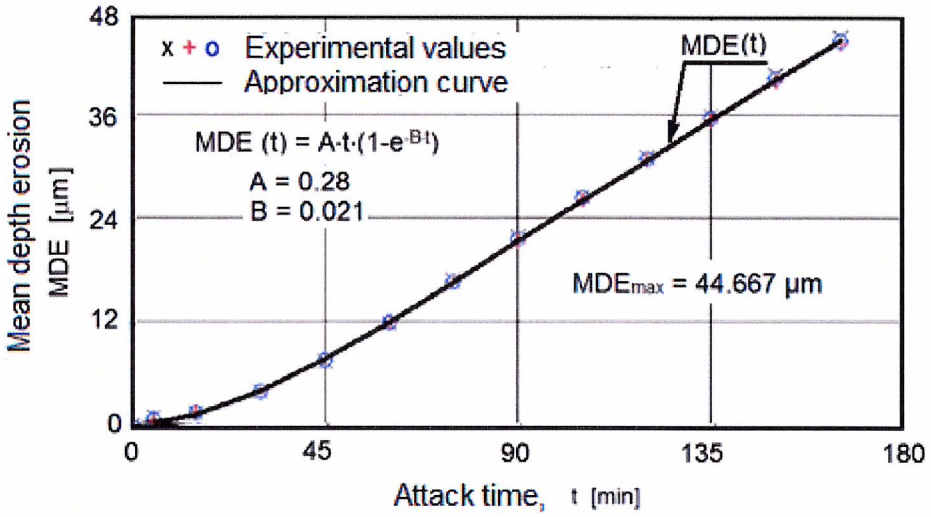

Fig.4.53 Evolution of mean depth erosion against cavitation exposure time

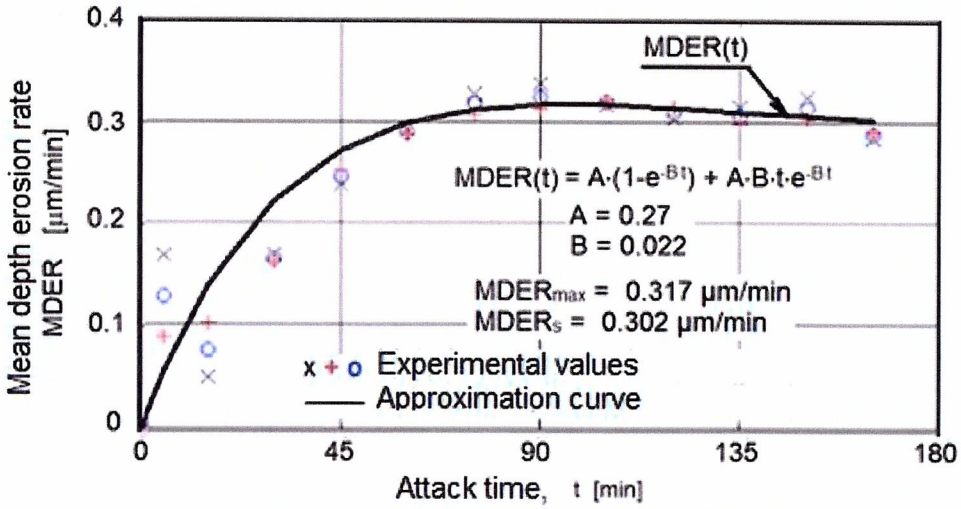

Fig.4.54 Evolution of mean depth erosion rate against cavitation exposure time

The evolution of the mean depth of penetration rate, in relation to the duration of the cavitation test, in terms of its expansion in the exposed sample area, is visible in the macroscopic images, captured with a camera at significant intervals (fig. 4.57), while the degree of damage and penetration in the structure of the material is shown in the SEM image, accompanied by the macroscopic image (fig. 4.58).

Min 15 Min 90 Min 135 Min 165

Fig.4.56 Images of specimen surface at different cavitation exposure time (**Sample 2**)

Sample 1 **Sample 2** **Sample 3**

Fig.4.57 Macroscopic images (taken with a Canon A480 camera) of the surfaces eroded by vibratory cavitation, after 165 minutes of cavitation exposure

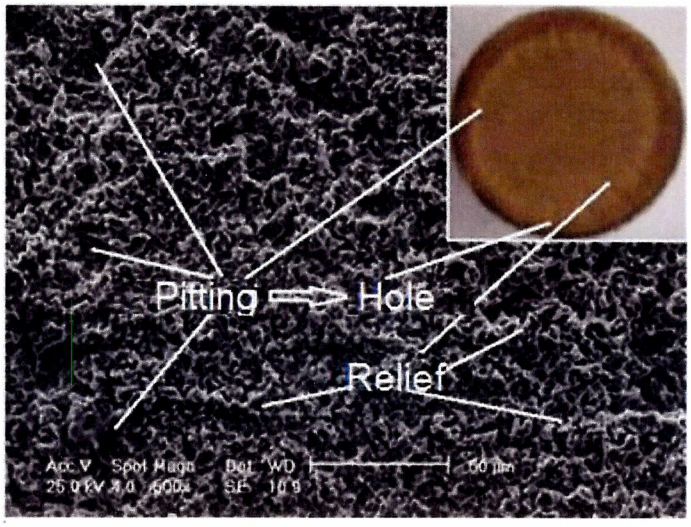

Fig.4.58 SEM and macroscopic images of the eroded microstructure, after a 165 minute exposure to cavitation –**Sample 2**

The bar chart from fig. 4.59 and the values for the three characteristic parameters (R_a, R_z and R_t), as recorded with the Mitutoyo analyzer, are in line with the macroscopic aspect of the sample surfaces from fig 4.56 and 4.57, as well as with the SEM image from fig. 4.58, thus showing the erosion propagation into the sample microstructure.

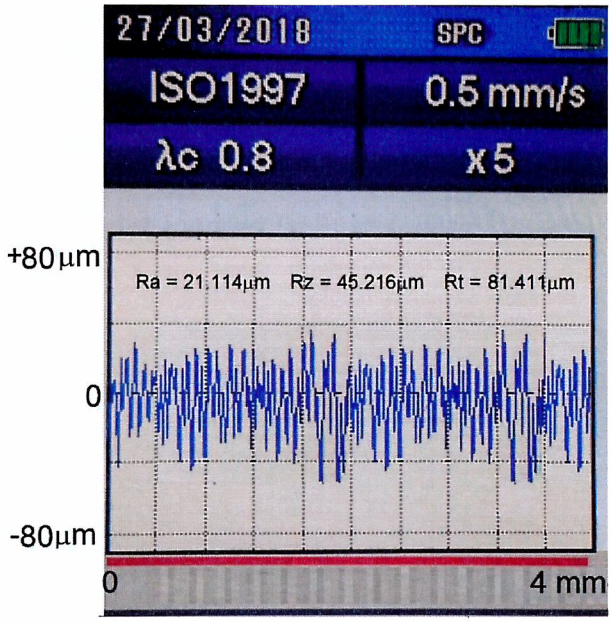

Starea 700-250

Fig. 4.59 Roughness parameters and profile registered with the Mitutoyo SJ 201 P device **(Sample 2)**

The heat treatment of tempering at 250°C, with slow cooling in air, causes a slight thermal stress-relief in the material and an onset of precipitation of secondary phases (fig. 4.61a). Bronze hardness does not decrease significantly, and therefore the cavitation-eroded surface shows characteristics similar to the structural state obtained as a result of the hardening at 700°C and empering in water (fig.4.61 b, c).

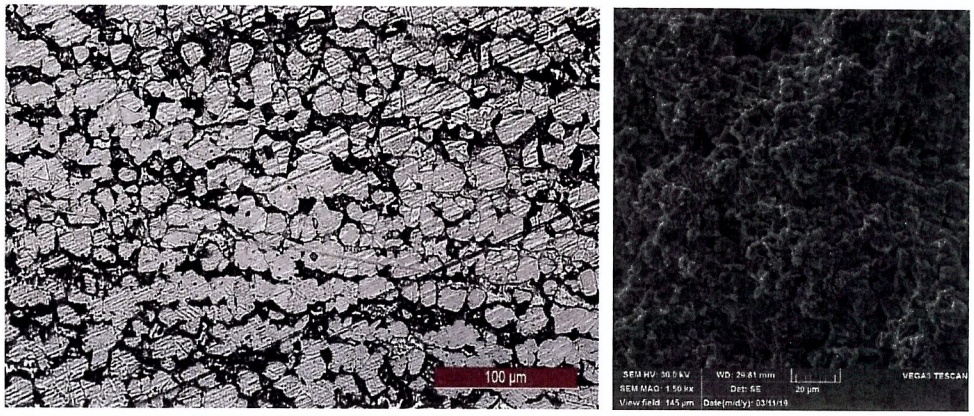

-a - -b-

Fig.4.61 Macroscopic image (a) and SEM image SEM (b), after a 165 minute exposure to cavitation

In-depth hardening starting at 700°C, with tempering at 500 °C

Figures 4.62 and 4.63 exhibit the experimental values for the three samples, as well as their analytically-built mediation curves.

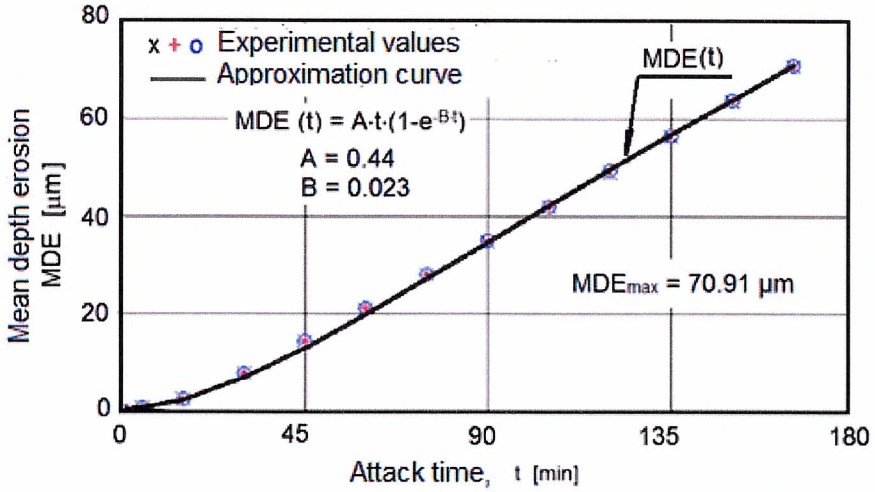

Fig.4.62 Evolution of mean depth erosion against cavitation exposure time

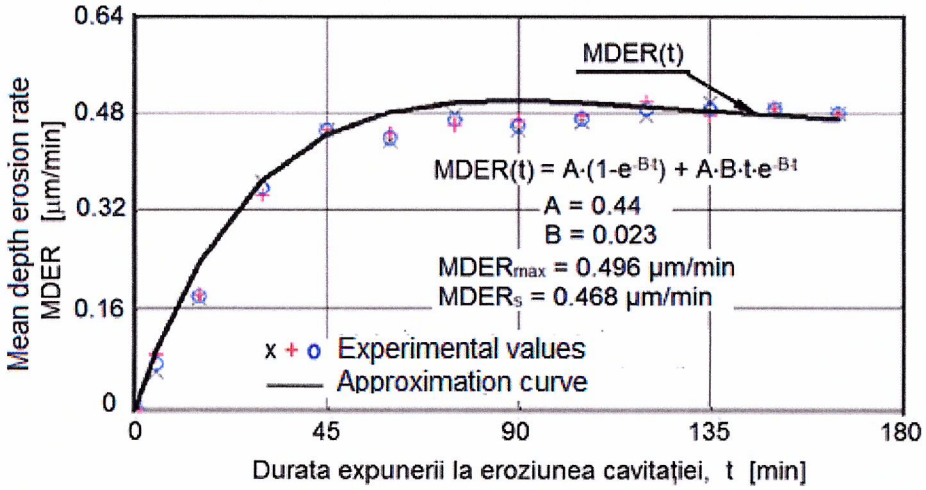

Fig.4.63 Evolution of mean depth erosion rate against cavitation exposure time

The expansion of the cavitation erosion in the exposed surface, during the attack, is illustrated by the photographs (macroscopic images) from fig. 4.65 (only valid for sample 2), and the crevice formation is illustrated in the images from fig. 4.66 and 4.67.

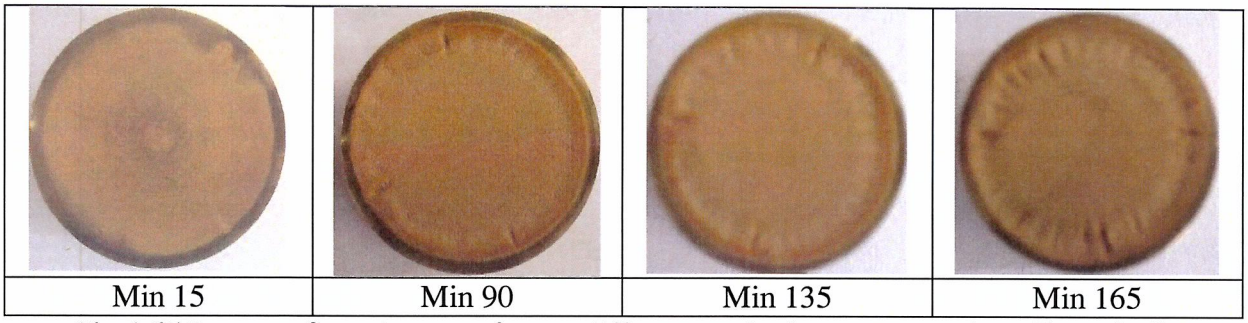

Min 15	Min 90	Min 135	Min 165

Fig.4.65 Images of specimen surface at different cavitation exposure time (**Sample 2**)

Sample 1 **Sample 2** **Sample 3**

Fig.4.66 Macroscopic images (taken with a Canon A480 camera) of the surfaces eroded by vibratory cavitation, after 165 minutes of cavitation exposure

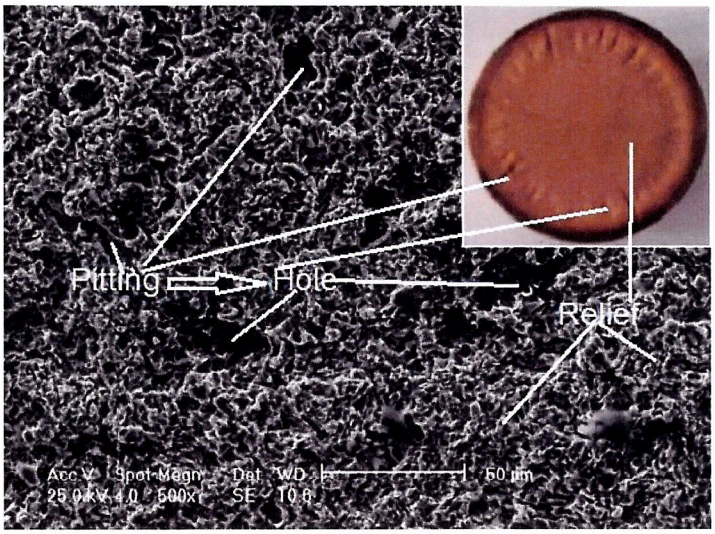

Fig.4.67 SEM and macroscopic images of the eroded microstructure, after a 165 minute exposure to cavitation – **Sample 1**

Fig. 4.68 shows the bar chart and the values for the three characteristic parameters (R_a, R_z and R_t), as recorded with the Mitutoyo analyzer on the sample identified as Sample 2.

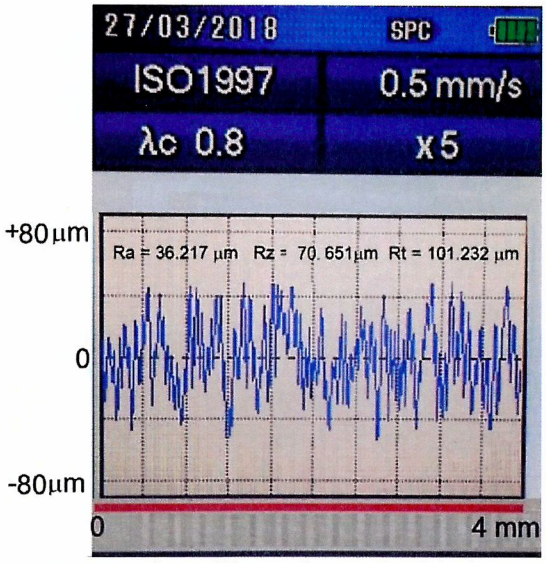

Fig.4.68 Roughness parameters and profile registered with the Mitutoyo SJ 201 P device (**Sample 2**)

The increase in the tempering temperature to 500°C results in a slight increase in the dimensions of the precipitated phases (fig. 4.70 a) and, as a consequence, in a relatively small decrease of the toughness and resistance to cavitation. The investigation under SEM of the sample surface subject to cavitation shows the formation of irregular micro-craters as a result of the expulsion of the precipitated secondary phase particles from the super-saturated β-phase solid solution, as well as the propagation of the cracks occurring mainly in the grain boundary areas (fig. 4.70 b).

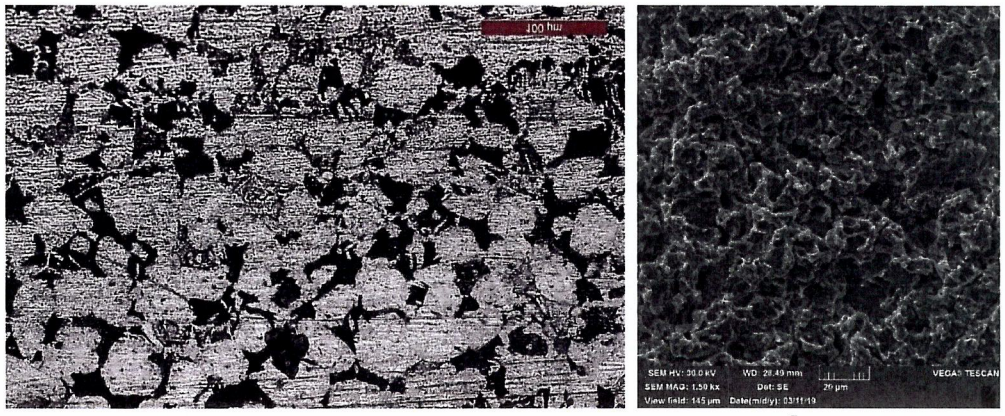

-a - **-b-**

Fig.4.70 Macroscopic image (a) and SEM image SEM (b), after a 165 minute exposure to cavitation

4.2.3. Comparison of the research results

The quantitative assessment of the resistance obtained after each of the three cycles, in comparison with the control state, is shown by the bar chart from fig. 4.75.

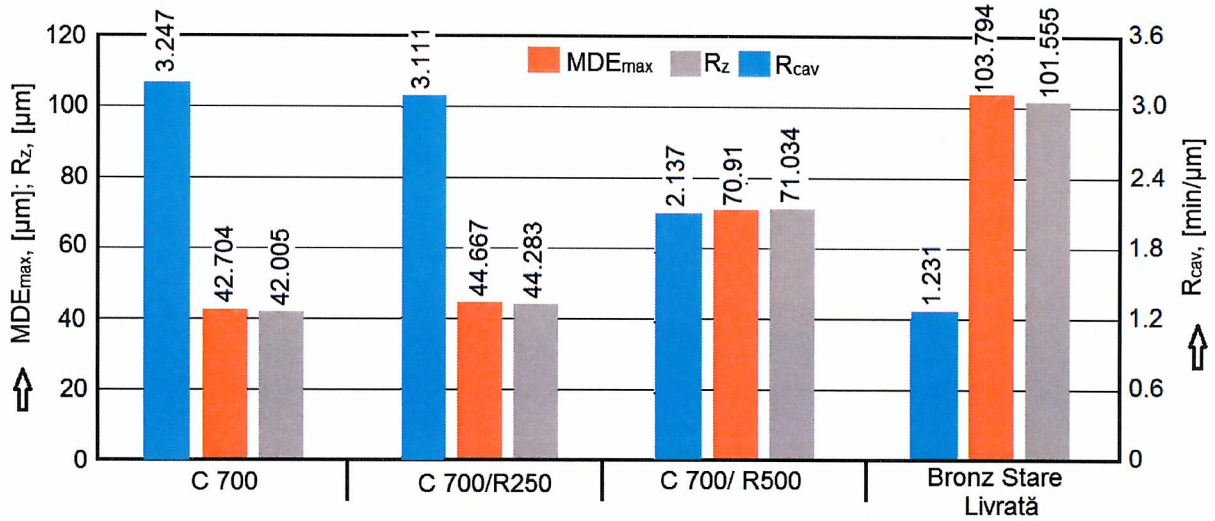

Fig.4.75 Histogram of estimation of resistance to erosion of cavitation (comparison of the heat treatment regimes)

The comparative data from the bar chart (fig. 4.75) show visibly inferior values for the mean roughness, R_z (as measured with the Mitutoyo analyzer and calculated according to the method described above), as well as for the maximum depths, MDE_{max}, while the parameter for cavitation resistance, R_{cav}, is visibly higher; these values were obtained after the three hardening cycles, and the hardening and tempering cycle respectively, were performed.

The bar chart from fig. 4.76, where we compare the values of the cavitation-erosion parameters for the 4 heat treatments used on brass (CuZn39Pb), and for the 3 heat treatments used for bronze (CuSn12-C), respectively, shows, without a doubt, that a resistance to cavitation-erosion can be achieved by in-depth heat treatments.

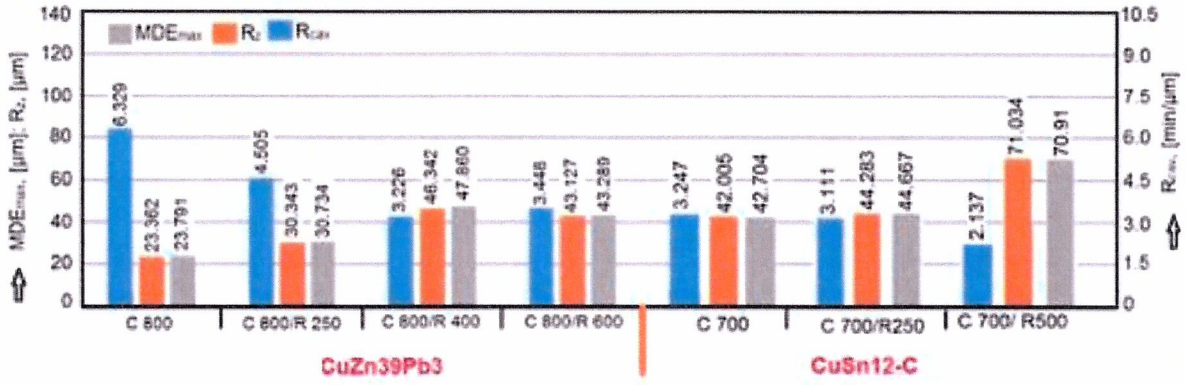

Fig.4.76 Histogram of estimation of resistance to erosion of cavitation (comparison of the heat treatment regimes - CuZn39Pb3 vis avis CuZn12-C)

The quantitative assessment of the resistance to cavitation-erosion, achieved after the application of the three heat treatments, is given by the values of the parameters MDE_{max} and R_{cav} from the bar chart in fig. 4.79.

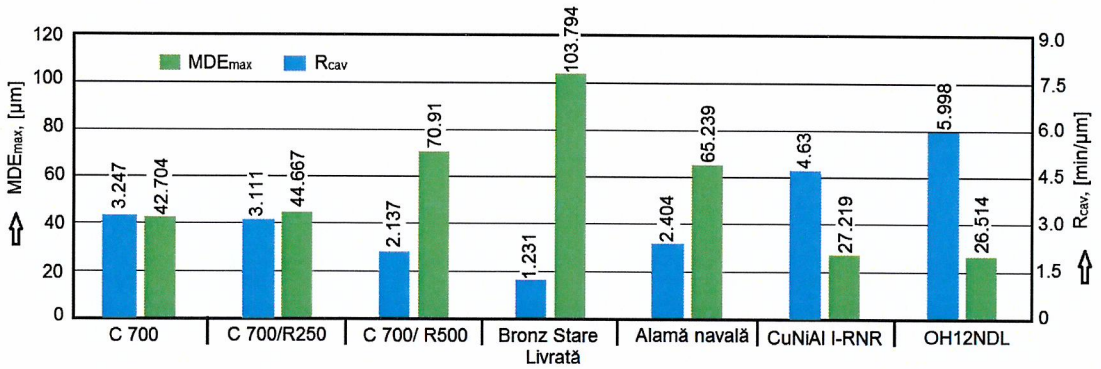

Fig.4.79 Histogram of estimation of resistance to erosion of cavitation (comparison with the standard materials)

The bar chart shows the upper values for the maximum erosion depth MDE_{max}, as well as the lower values of the cavitation resistance R_{cav}, in comparison with the values pertaining to the marine-grade bronze (CuNiAl I-RNR) (MDE_{max} = 21.219 µm, R_{cav} = 4.63 min/µm) and with the values pertaining to stainless steel (OH12NDL) (MDE_{max} = 26.514 µm, R_{cav} = 2.404 min/µm).

4.3 Conclusions

Albeit there are certain differences, determined by the structure of bronze and the surface toughness, achieved after the application of the in-depth heat treatment, the results are similar to the heat-treated brass.

- The comparison with the control materials, i.e. stainless steel (OH12NDL) and marine-grade bronze (CuNiAl I-RNR), has shown that, regardless of the treatment applied, the resistance to cavitation erosion decreases less in the case of the hardening treatment, and the most in the case of the hardening followed by tempering at 500°C.
- The comparison with the initial-state samples confirms that the in-depth heat treatments remain a solution to increase the resistance to cavitation erosion;
- The investigations performed by comparison with the control materials, i.e. stainless steel OH12NDL, marine-grade bronze CuNiAl I-RNR, and marine-grade brass, confirm that bronze CuSn-C, after it has gone through hardening or hardening + tempering heat treatments, may be used for the manufacture of parts subject to cavitation currents, such as pipe fittings, stoppers and valves mounted on forced-fit piping, the rotors of high-volume pumps, and even the ship propellers.

5. TECHNIQUES AND MATERIALS USED IN THE SURFACE PROTECTIVE COATING OF PARTS SUBJECT TO CAVITATION

The polymer-based mixtures have been used more and more frequently lately as protection layers and repair materials for the component parts subject to hydrodynamic stress (such as hydraulic equipment impellers and rotors, ship propellers, rings and disks used for valves mounted on forced-fit piping, for valve seats, as well as for the lining of pipes subject to erosion damage, etc.) [1-4, 7]. Based on the aspects mentioned above, this chapter presents the results of the research conducted on the behavior and resistance to the vibratory cavitation erosion of certain types of polymer mixtures (also known as polymer resins or modified polymers), applied on the metallic surface of the samples subject to cavitation, made out of the bronze used to manufacture component parts prone to cavitation damage, such as [9, 11, 7]: valve seats, ship propellers, butterfly valve rings.

5.I. Modified polymeric mixtures

In order to research the behavior of the modified polymers to vibratory cavitation, we have used samples (fig. 5.1) taken from the bronze (CuSn12 - C) used in the previous experiments.

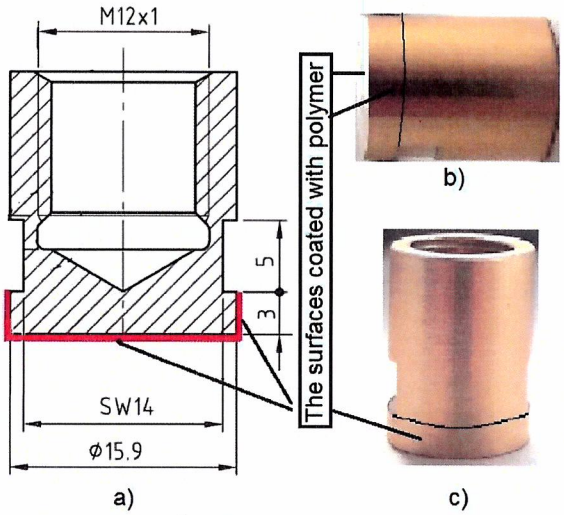

Fig. 5.1 Sample image
a) - sample section; b) şi c) - real sample

We have studied 5 types of polymer resins, and two samples were tested for each type.

The test results showing the resin behavior to vibratory cavitation

The images below show the way in which resins behave to the strain generated by vibratory cavitation.

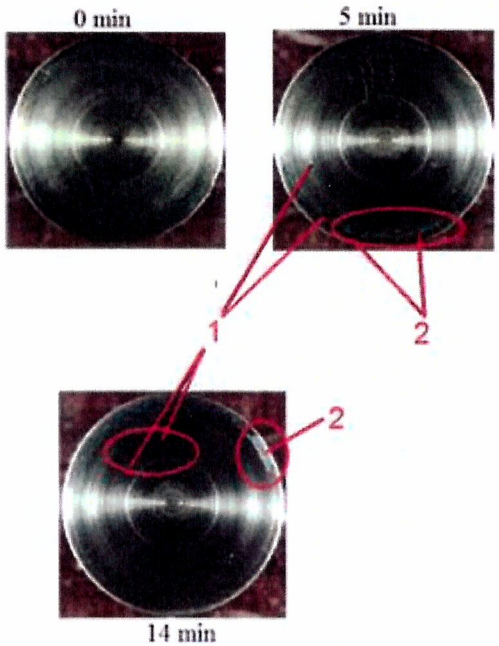

Fig.5.17 Behavior evolution to vibratory cavitation of the mixture typ 1 deposited on the flat surface of the sample
1. perforations of the mixturer (cracks/pits); 2. detached mixture film and bubbles with small dimensions

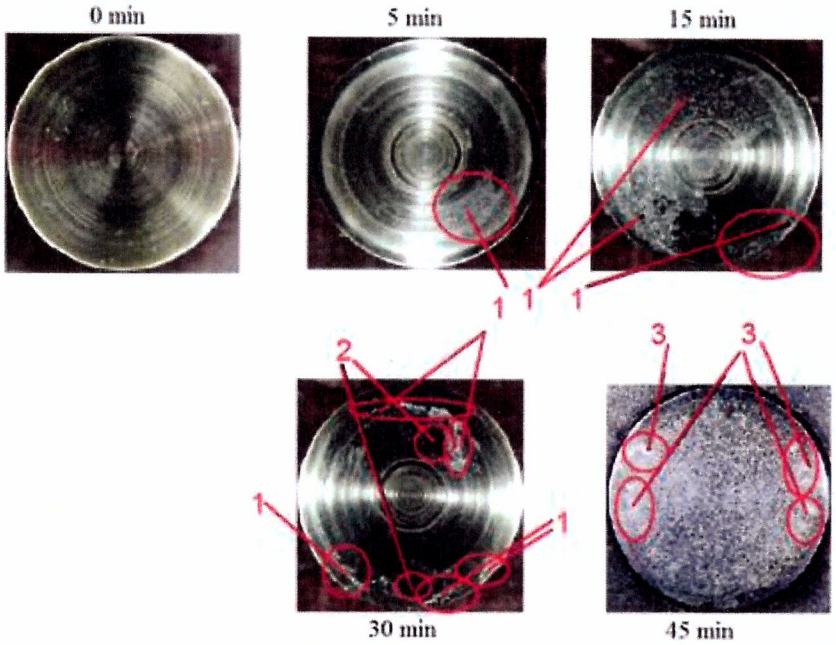

Fig.5.20 Behavior evolution to vibratory cavitation of the mixture layers typ 2 deposited on the flat surface of the sample

1. detached mixture film and bubbles with small dimensions; 2. the area remaining after the mixture film expelled; 3.cracks/pits

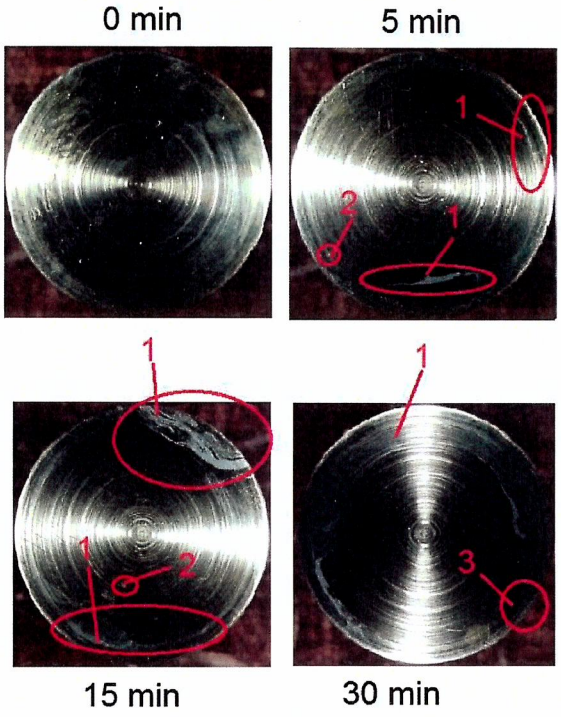

Fig.5.21 Behavior evolution to vibratory cavitation of the mixture layers typ 3 deposited on the flat surface of the sample

1. water and bubbles between the polymer film and the metal surface of the sample; 2. perforations in the polymer film; 3. erosion in the metallic surface (cracks/pittings).

Fig.5.22 Behavior evolution to vibratory cavitation of the mixture layers typ 4 deposited on the flat surface of the sample.

1- water and bubbles between the polymer film and the metal surface;
2- perforations in the polymer film; 3- erosions in the metallic surface (cracks/pittings)

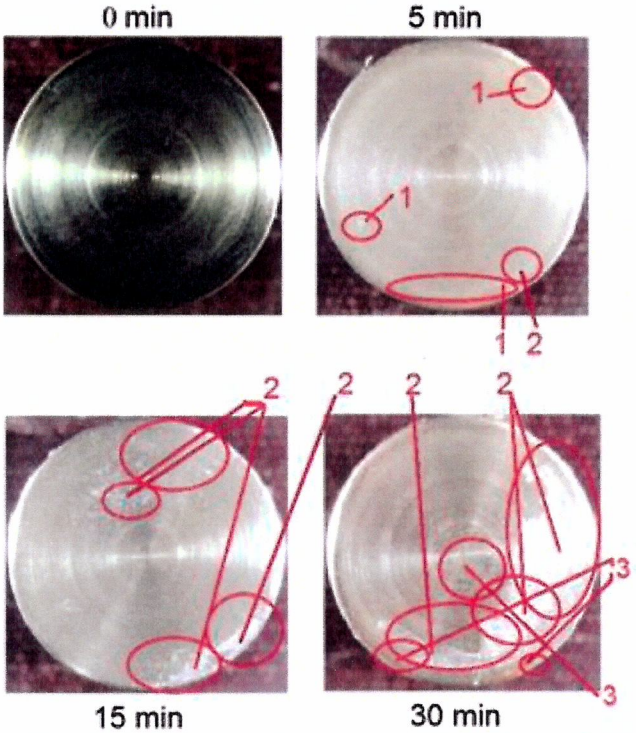

Fig.5.24 Behavior evolution to vibratory cavitation of the mixture layers typ 5 deposited on the flat surface of the sample

1. perforations in the polymer film; 2. water and bubbles between the polymer film and the metal surface of the sample; the remaining polymer film fixed on the metal surface; 3. cracks/pittings

Conclusions

1. The flaking of the mixture coating, in thin layers, shows that it is indeed elastic and tear-resistant, yet further improvement is needed in terms of technology, that will ensure enhanced resin adhesion to the metal surface, i.e. the copper-based alloy (bronze CuSn12), so that the resin layer does not detach and perforate under the shocks caused by the cavitation microjets.

4. The results have proved that further research is needed in order to create polymer resins with increased resistance to cavitation erosion, so that they can be used to coat the hydraulic equipment impellers, the ship propellers and other component parts subject to severe cavitation, the repairs of which take time and cost much money.

5. II. Copper-based coating, applied by HVOF thermal spraying

The thermal spraying has been extensively used in the aerospace, automotive and ship-building industries, due to its numerous advantages [25], when compared to other similar processes (molten metal hot-dip coating, diffusion, plating, galvanic coating).

Four types of copper-based powders were used in the experiment, with the chemical compositions and densities displayed in table 5.1.

These powders were applied on the circular surfaces of the samples subject to cavitation, made out of carbon-steel 270-480 W Sr ISO 13755:1995.

Table 5.1. Chemical composition of the powders used

Specimen	Chemical composition [% masă]										ρ [g/cm^3]
	Co	Cr	Cu	Fe	Mo	Ni	Pt	Sn	Ti	Zn	
1	-	-	95.96	-	0.02	-	-	4.02	-	-	8.85
2	-	-	96	-	-	-	-	4.0	-	-	8.85
3	0.34	7.6	44.7	0.25	0.17	18.63	0.24	-	0.37	27.7	8.30
4	0.27	6.64	47.08	0.22	0.17	16.2	0.27	-	0.32	28.83	8.31

Table 5.2 shows degradation images of the coated surface, after various cavitation erosion intervals.

Table 5.2 Macro images of the degradation of the deposited layer

Speci-men	Attack time [min] 1	5	30	60	90
1					
2					
3					
4					

Fig. 5.34 shows the evolution in volume loss which, due to the approximately identical thicknesses (≅ 0.8 mm), represents a percentage indication of the coating expulsion from the surface subject to cavitation, with a 15.8 mm in diameter. In order to better show the resistance achieved by using these coatings, the diagram also shows the volume loss in the base 270-480 W steel.

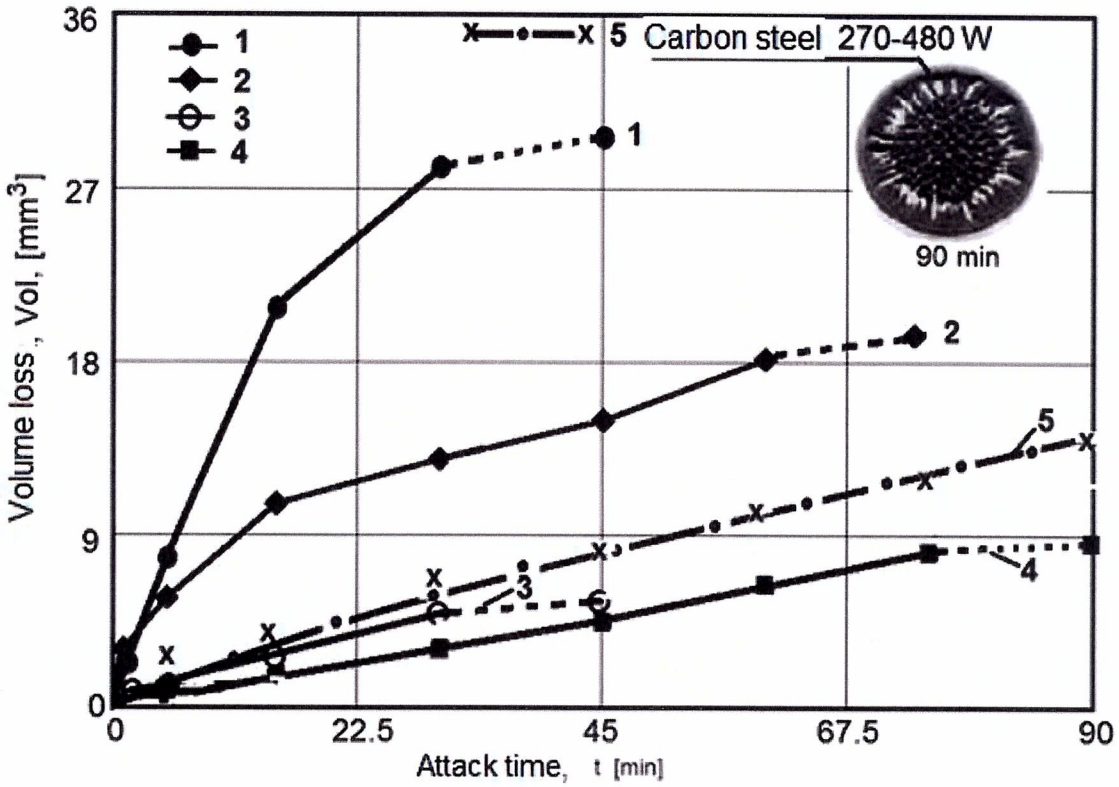

Fig.5.34 Evolution of the volume losses of the layers deposited by thermal spray

Conclusions

The resistance of the thermal spray coating to the cavitation damage caused by the microjets produced by bubble collapsing, as created by the linear vibrations in the vibrating piezoelectric crystal assembly, is closely linked to the nature of the material used (chemical composition and density).

After comparing the resistance of the 4 layers with the resistance of steel 270-480 W Sr ISO 13755:1995, it was noted that certain types of polymer resin, highly adhesive to the surfaces subject to cavitation, can significantly increase the resistance of component parts to cavitation-erosion attacks, thus having a positive effect on their life cycle.

6. FINAL CONCLUSIONS AND ORIGINAL CONTRIBUTIONS. NEW RESEARCH PERSPECTIVES (*SELECTED*)

The ample research in the specialty literature, the experimental investigations and the assessments performed during the Ph.D program and presented in this Ph.D thesis, have led to the following **general** conclusions regarding the cavitation tests performed using vibratory equipment:

- the research of cavitation-erosion remains a current issue that has gained momentum in the last few years, as there are increasingly more and more problems in the operation of

equipment subject to cavitation, i.e. impaired performance and shortened duration of continuous operation;
- the mechanisms causing cavitation-erosion have not been entirely unraveled, due to a multitude of factors defining the flow dynamics and because there are still no materials or treatment technologies that can create surfaces or structures which are perfectly resistant to the impact of microjets formed by cavitation bubble implosion.
- the investigation of cavitation-erosion in the laboratory is the best method applicable, as the test duration is short and there are similarities between the mechanical degradation mechanism (i.e. the propagation of fatigue cracks, at a microscopic scale, in all the structure) and the processes occurring in the industrial equipment, even if the parameters defining the cavitation hydrodynamics are completely different;
- for the assessment of the behavior of materials to cavitation-erosion, it indicated to use the specific curves, the characteristic parameters and micro-photographs of the degraded surfaces, taken at intermediary intervals and at the end of the cavitation attack;

Personal and original contributions
- the ample research of specialty literature in order to learn the mechanics of the cavitation-erosion and the development of the knowledge needed to provide explanations, by making comparisons with the already published results, of the behavior and resistance to cavitation-erosion of the two copper-based alloys, in initial delivered state and after the application of heat treatments;
- provide a reason to continue using the in-depth heat treatments in order to increase the resistance to cavitation-erosion, obtained by the changes in the material structure and properties;
- provide proof that the resistance and behavior of brass and bronze are closely related to the parameters of the heat treatment applied, the micro-structure, the chemical composition, and the mechanical properties, especially the toughness of micro-structures.

New research perspectives
- the investigation of other copper-based alloys, which have different physical and mechanical properties, which could cost less, and which could acquire superior characteristics with respect to the behavior and resistance to cavitation-erosion, through the use of various types of coatings and treatments;
- the study of the variation in the toughness of the micro-structure subject to cavitation, in relation to the duration of the vibratory cavitation test;
- opportunities to improve the cavitation resistance of copper alloys by using welding techniques and coatings with various powders;
- the research of the types of bronze and brass used to manufacture fresh-water ship propellers;
- further research regarding other types of polymer resins and methods aimed at increasing their adhesion to the surface subject to cavitation.

As a final conclusion, this PhD project is a bridge between mechanical engineering and materials engineering and it follows the current research trend, i.e. to find new solutions to increase the life cycle of equipment subject to mechanical strain caused by cavitation.

REFERENCES (SELECTED)

1. Anton I., Cavitatia, Vol I, Editura Academiei RSR, Bucuresti, 1984

2. Anton I., Cavitatia, Vol II, Editura Academiei RSR, Bucuresti, 1985
3. Bordeaşu I., Eroziunea cavitaţională a materialelor, Editura Politehnica, Timişoara, 2006
4. Bordeaşu I., Teză de doctorat: Eroziunea cavitaţională asupra materialelor utilizate în construcţia maşinilor hidraulice şi elicelor navale. Efecte de scară, Timişoara, 1997
5. Bordeasu, I., Oanca, O., Considerations Regarding the Cavitational Damage Process on Bronze and Brass Used in the Marine Screw Manufacture, Machine Design, Vol.3(2011) No.4, ISSN 1821-1259 pp. 277-280, 2011
6. Bordeaşu, I., Anton, M.I.,Correlation Between Cavitation Rate with Both Parameters of the 6. Vibratory Apparatus and the Phisico-mechanical Properties of the Material, Third International Symposium on Cavitation, Grenoble, 7-10 April, France, p. 199-202, 1998
7. Bordeaşu I., ş.a., An Analytical Model for the Cavitation Erosion Characteristic Curves, Scientific Bulletin "Politehnica" University of Timişoara, Transaction of Mechanics, Tom 49(63), ISSN:1224-6077, Timişoara, p.253-258, 2004
8. Breslin, J.P., Andersen P., Hydrodynamics of ship propellers, 3, Editor Cambridge University Press: United Kingdon, 2003
9. Brooks J. W. Thèse de doctorat (Ph. D.). Universitè de Birmingham, 1987
10. Carlton, J., Marine propellers and Propulsion, Elsevier Ltd: Oxford, 2007
11. Franc J P, Kueny J L, Karimi A, Fruman D H, Fréchou D, Briançon-Marjollet L, Yves Billard J Y, Belahadji B, Avellan F and Michel J. M., *La cavitation. Mécanismes physiques et aspects industriels*, Press Universitaires de Grenoble, Grenoble, France, 1995
12. Garcia R., Hammitt F. G., Nystrom R.E., Corelation of cavitation damage with other material and fluid properties, Erosion by Cavitation or Impingement, ASTM, STP 408 Atlantic City, 1960
13. Geru N., s.a.., Analiza structurii materialelor metalice, Editura Tehnică, Bucureşti, 1991
14. Geru, N., Metalurgie fizică, Editura didactică şi pedagogică, Bucureşti, 1981
15. Hobbs J.M., Experience with a 20 – KC Cavitations erosion test, Erosion by Cavitations or Impingement, ASTM STP 408, Atlantic City, 1960
16. Hobbs J.M., Vibratory cavitation erosion testing at nel, Confernce Machynery Groop, Edinburgh, 1974
17. Jurchela, A.D., Cercetări asupa eroziunii produse prin cavitaţie vibratorie la oţelurile inoxidabile cu conţinut constant în crom şi variabil de nichel, Teza de doctorat, Timişoara, 2012
18. Karabenciov A.,. Cercetări asupra eroziunii produse prin cavitaţie vibratorie la oţelurile inoxidabile cu conţinut constant în nichel şi variabil de crom, Teza de doctorat, Timişoara, 2013
19. Karimi A., Heuze J.L., - Erosion de cavitation d' alliages amortissants a base de magnese et de cuivre, La Houille Blanche, Nr. 7/8 – 1992
20. Meigh, H.J., Cast and wrought aluminum bronzes properties, processes and structure, Cambridge: IOM Communications Ltd, University Press, 2000
21. Mitelea I., - Studiul metalelor, Litografia Institutului Politehnic"Traian Vuia" Timisoara, 1983
22. Mitelea I 2009 *Materiale inginereşti,* Editura Politehnica, Timişoara, Romania
23. Okada, T., Iwai, Z., Hattori, s., Tanimura, N., Relation between impact load and the damage produced by cavitation bubble collapse, Wear 184, 1995, p.231-239

24. Popoviciu M., Bordeaşu I., A standard material for cavitation erosion tests, Hydraulic Machinery and Hydrodinamics, Vol II, Timişoara, 1994
25. Popoviciu O.M., Bordeaşu I., Tehnologia fabricaţiei sistemelor hidraulice, Editura Politehnica, Timişoara, 1998
26. Steller J. K., International cavitation erosion test – test facilities and experimental results, 2 – emes Journees Cavitation, Paris, March, 1992.
27. Thiruvengadam A., Preiser H. S., - On testing materials for cavitation damage resistence,Report. 233 – 3, 1963.
28. ***Standard method of vibratory cavitation erosion test, ASTM, Standard G32, 2010
29. ***www.sciencedirect.com.Zheng Y.G., Luo S.Z., Ke W., Cavitation erosion–corrosion behaviour of CrMnB stainless overlay and 0Cr13Ni5Mo stainless steel in 0.5M NaCl and 0.5M HCL solutions,
30. ***www.sciencedirect .com: Cuppari M.G. Di V., Souza R.M., Sinatora A., Effect of hard second phase on cavitation erosion of Fe–Cr–Ni–C alloys
31. *** http://www.uni-duisburg.de/FB7/IST/links/Klassif.html], Uni-Duisburg FB IST: Liste der Klassifikationsgesellschaften und Organisationen
32. *** http://www.ampcometal.com/common/datasheets/us/A45_EX_E_US.pdf
33. *** http://www.ampcometal.com/common/datasheets/en/AM4_EX_E.pdf
34. ****www.sulzer.com/as/-/media/.../TS_MaterialGuide_EN_052012.pdf*,Thermal Spray Materials Guide
35. https://copperalliance.ro/despre-cupru/cupru-si-aliaje-de-cupru/aliaje//..
36. http://www.scritub.com/stiinta/chimie/Utilizarea-metalelor-si-a-alia1621615721.php
37. Registrul Naval Roman, Reguli pentru clasificarea si constructia navelor maritime, 1995.
38. https://www.inspection-for-industry.com/pump-net-positive-suction-head-test.html
39. https://jacpump.wordpress.com/2011/04/17/solving-a-cavitation-problem
40. https://www.google.ro/search?biw=1280&bih=913&tbm=isch&sa=1&ei=xSvoW7jRKsX9kwW3p6WIAg&q=cavitation+empeller&oq=cavitation+empeller
41. https://www.ogorul.ro/p/pompa-de-transvazare-din-bronz-debit-33-litriminut-tp200
42. https://www.tehnocenter.ro/cm-40-200-b-pentax-pompa-de-suprafata-putere-5-5-kw-inaltime-de-refulare-44-9-27-9-m-debit-maxim-150-700-l-
43. https://www.emag.ro/pompa-de-apa-pentax-csb-150-pentru-irigatii-prin-inundare-si-picurare-230-v-inaltime-max-de-refulare-21-5-m-debit-max-400-l-min-2-pentaxcsb150/pd/DMXBW2BBM/]
44. https://ispshop.ro/collections/pompe/products/pompa-n20- tellarini?variant = 375237 34607]
45. https://www.inspection-for-industry.com/pump-net-positive-suction-head-test.html
46. http://www.lnt-hydraulics.com/hydraulic-products/radial-piston-pumps/
47. http://www.directindustry.com/prod/spitznas/product-190535-1872759.html
48. https://www.google.ro/search?biw=1280&bih=913&tbm=isch&sa=1&ei=cS3oW_zHIsewkwXzorQY&q=vane+bronz&oq=vane+bronz&gs_l]
49. Lazar, I., Bordeasu, I., Popoviciu, M. O., Mitelea, I., Craciunescu, C. M., Pirvulescu, L. D., Sava M., Micu L. M., Evaluation of the brass CuZn39Pb3 resistance at vibratory cavitation erosion, International conference on applied sciences ICAS2018, May 9-11, Banja Luka, Bosnia Hertegovina, 2018
50. [http://www.sim.tuiasi.ro/wp-content/uploads/Carcea-Aliaje-Neferoase-de-turnatorie1.pdf,-Carcea, I, Gherghe, M, Aliaje Neferoase De Turnătorie]

51. https://www.google.ro/search?biw=1280&bih=864&tbm=isch&sa=1&ei=G7f6W_qtF5CakwWHiqXADQ&q=tin+bronze+microstructure&oq=bronze+microstructure&gs_l=img.1.1.0i19j0i5i30i19l4.11445.17645..20508...0.0..0.85.1433.21.....1....1..gws-wiz-img.....0j35i39j0i67j0i30j0i8i30i19.F8pu5W7Eo2w]
52. Ghera, C., Rolul tratamentelor duplex în creşterearezistenţei la cavitaţie a oţelurilor pentru aparatura sistemelor hidraulice, Teza de doctorat, Timisoara, 2017
53. Salcianu, L., Curgerea în vanele fluture și eroziunea prin cavitaţie a componentelor din oţeluriinoxidabile austenitice Teza de octorat, Timisoara, 2017
54. Oanca O., Tehnici de optimizare a rezistenţei la eroziunea prin cavitaţie a unor aliaje CuAlNiFeMn destinate execuţiei elicelor navale, *Teza de doctorat*, Timișoara, 2014
55. *** http://www.kleinmetals.ch/shop/Datenblatt/E/631.pdf
56. Küçükömeroğlu T and Kara L 2014 The friction and wear properties of CuZn39Pb3 alloys under atmospheric and vacuum conditions, *Wear*, 309, pp 21–28
57. https://www.rna.ro/Legislatie/SCTN/Norme%20ANR%20scanate/2-1Inspectarea%20 si%20repararea%20elicelor.pdf
58. Bordeasu, I., Popoviciu, M. O., Ghera, C., Micu, L. M., Pirvulescu, L. D., Bena, T., The use of Rz roughness parameter for evaluation of materials behavior to cavitation erosion, International Conference on Applied Sciences (ICAS2017), IOP Conf. Series: Materials Science and Engineering 294 (2017) 012020 doi:10.1088/1757-899X/294/1/012020, Hunedoara, 2017
59. Bordeaşu I., Popoviciu M.O., Patrascoiu C-tin, Bălăsoiu V.: „An Analytical Model for the Cavitation Erosion Characteristic Curves", Scientific Buletin Politehnica University of Timisoara, Transaction of Mechanics, Tom 49(63), Timişoara, ISSN:1224-6077, pp. 253-258, 2004
60. https://www.animavision.ro/pompa-hidrofor-elpumps-jpv-1300b-rotor-bronz-p-4564.html